Recent Advances in Biointegrated Optoelectronic Devices

Huihua Xu, Lan Yin, Chuan Liu, Xing Sheng,* and Ni Zhao*

With recent progress in the design of materials and mechanics, opportunities have arisen to improve optoelectronic devices, circuits, and systems in curved, flexible, stretchable, and biocompatible formats, thereby enabling integration of customized optoelectronic devices and biological systems. Here, the core material technologies of biointegrated optoelectronic platforms are discussed. An overview of the design and fabrication methods to form semiconductor materials and devices in flexible and stretchable formats is presented, strategies incorporating various heterogeneous substrates, interfaces, and encapsulants are discussed, and their applications in biomimetic, wearable, and implantable systems are highlighted.

1. Introduction

Optoelectronic devices, either inorganic or organic materials based, are electronic and optical devices that emit, guide, modulate and receive light. Advanced optoelectronic devices including light-emitting diodes (LEDs), lasers, solar cells, and photodetectors have been extensively explored for various applications in fields such as energy, communication, and healthcare. Recently, significant attention has been brought to the integration of customized optoelectronic devices and biological systems, and as a result, researchers have turned their focus to advancing bioinspired and biointegrated materials and devices that offer not only fundamental impact on light–matter interactions at biointerface but also new opportunities for sensing, diagnostics, and therapeutics.[1,2]

Dr. H. Xu, Prof. C. Liu
State Key Laboratory of Optoelectronic Materials and Technologies
Guangdong Province Key Laboratory of Display Material and Technology
School of Electronics and Information technology
Sun Yat-Sen University
Guangzhou 510275, China
Dr. H. Xu, Prof. N. Zhao
Department of Electronic Engineering
The Chinese University of Hong Kong
New Territories, Hong Kong SAR, China
E-mail: nzhao@ee.cuhk.edu.hk
Prof. L. Yin
School of Materials Science and Engineering
Tsinghua University
Beijing 100084, China
Prof. X. Sheng
Department of Electronic Engineering
Tsinghua University
Beijing 100084, China
E-mail: xingsheng@tsinghua.edu.cn

The ORCID identification number(s) for the author(s) of this article can be found under https://doi.org/10.1002/adma.201800156.

Conventionally, high-performance optoelectronic devices are based on single-crystalline inorganic semiconducting materials such as silicon (Si) and gallium arsenide (GaAs), with active device structures grown and formed on hard, rigid, flat, bulky, and highly stable crystal substrates. By contrast, biosystems are typically soft, curvilinear, flexible, stretchable and temperature sensitive. The structural and property mismatch between conventional devices and biosystems imposes significant challenges for reliable biointegration, thus limiting the applicability of existing optoelectronic devices in biomedical fields. Therefore, the need has emerged to enhance the design, mechanics, and the fabrication of high-performance optoelectronic devices, circuits, and systems in curved, flexible, stretchable, and/or biocompatible format, while opportunities for improved biointegrated optoelectronic platform arise at the same time.[3–6]

Here, we first review the inorganic and organic semiconductor materials that have been explored for biointegrated optoelectronics applications. Then, we present the strategies to introduce flexibility or stretchability to these materials. We also review the overall device design from the perspective of substrate selection, interface engineering, and encapsulation, followed by the strategies for fabricating devices that are highly flexible, stable, and conformal to skin, while maintaining high performance. It is noted that recently there are significant advances in the development of new nanomaterials, perovskites, and inorganic/organic hybrid–based materials and devices that are promising for biointegration. Examples of reviews can be found in the recent literature,[7–9] which are beyond the scope of this paper. Finally, we provide examples of biointegrated optoelectronic devices in areas of biomimetic devices, implantable devices for neural applications, and wearable devices for cardiovascular monitoring.

2. Materials, Devices, and Systems

2.1. Semiconductor Materials

2.1.1. Inorganic Semiconductor Materials

To realize high-quality single-crystalline materials that endure standard wafer growth and micro/nanomanufacturing steps, inorganic (Si, GaAs, etc.) optoelectronic devices are typically formed on lattice-matched, thick semiconductor substrates. In order to integrate with flexible, stretchable, and/or biocompatible platforms, it is often inevitable to eliminate the original

**ADVANCED
SCIENCE NEWS**
www.advancedsciencenews.com

**ADVANCED
MATERIALS**
www.advmat.de

growth substrates so as to develop freestanding, thin-film, micro/nanoscale semiconductor membranes and devices. Indeed, reduced device thicknesses result in lower flexural rigidities, and hence improving bendability and conformal bonding to unusual curvilinear substrates.[4] However, conventional wafer thinning methods rely on chemical/mechanical polishing and/or dry etching, and neither of which is likely to reduce the device thickness to less than 10 μm. Moreover, removing growth substrates suggests a waste of raw materials and an increase in fabrication cost, which will place cost-competitive solar cells manufacturers in an extremely disadvantageous position. Therefore, it is of paramount interest to develop a reliable and effective process to exfoliate thin-film device layers (less than 10 μm) from single-crystalline substrates.

Table 1 summarizes different methods to form freestanding, single crystalline, and thin-film devices from the growth substrate. One common technique to separate the thin-film devices from the substrate is to form and then subsequently remove the "interlayer" or "sacrificial layer" between the active thin-film device layer and the substrate (**Figure 1**a). A typical example is the thin-film Si-based membranes and devices fabricated from the commercially available silicon-on-insulator (SOI) substrate. As shown in Figure 1b, the SiO_2 interlayer can be selectively removed by hydrofluoric acid (HF)-based solutions, and the top Si thin films can be then exfoliated (with a thickness down to 20 nm).[6,10] Note that HF etching selectivity between SiO_2 and Si is almost infinite. Similar approaches are employed to form crystalline semiconductor membrane-based devices from "XOI" substrates, in which "X" can be germanium (Ge), SiGe, silicon carbide (SiC), etc.[11–13] Another method to obtain the freestanding thin-film Si device is to start with {111}-oriented Si wafers and etch through the trenches along the ⟨110⟩ direction in potassium hydroxide (KOH)-based solutions (Figure 1c).[14,15] Combined with protected surfaces and sidewalls, anisotropic etching in KOH (etching selectivity along ⟨110⟩ and ⟨111⟩ is larger than 100:1) defines the geometries of the Si film being released. Similarly, for gallium nitride (GaN) and indium gallium nitride (InGaN) based thin-film devices grown on Si{111} wafers, KOH solutions isotropically etch along the Si⟨110⟩ direction and release GaN/InGaN thin-film LEDs from the Si substrate (Figure 1d).[16]

Optoelectronic devices based on III–V compound semiconductors are typically grown on lattice-matched substrates via methods such as metal-organic chemical vapor deposition or molecular beam epitaxy. During the growth process, a lattice-matched sacrificial layer can be inserted between the active device layer stack and the substrate, without affecting the material quality and device performance. Such sacrificial layer can be selectively removed (typically via wet etching), and thus releasing thin-film III–V devices from the growth substrate. For GaAs, indium gallium phosphide (InGaP) and aluminum indium gallium phosphide (AlInGaP)-based devices grown on GaAs substrates, aluminum gallium arsenide ($Al_xGa_{1−x}As$), or AlAs (when $x = 1$) are often used as the sacrificial layer to be fully lattice matched to GaAs at different Al concentrations ($0 < x < 1$). For AlGaAs with a high Al concentration ($x > 0.7$), a very high selectivity ($>10^5$:1) over GaAs or InGaP can be realized in HF solutions.[17–21] Figure 1e illustrates a multilayered GaAs/AlAs stack with AlAs layers partially undercut in HF.[20]

Huihua Xu is currently a research staff member in the School of Electronics and Information Technology at Sun Yat-Sen University. She received her Ph.D. degree in materials processing engineering from Nanjing University of Aeronautics and Astronautics. After graduation, she worked at the Chinese University of Hong Kong as a postdoctoral researcher and then joined Sun Yat-Sen University in 2017. Her research interests include organic electronics/optoelectronics for biomedical applications.
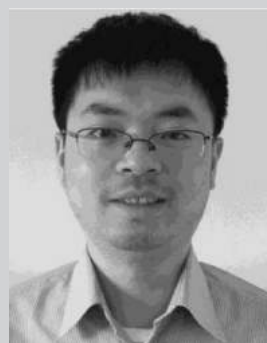
Xing Sheng is currently working as an associate professor in the Department of Electronic Engineering at Tsinghua University, China. He received his bachelor and Ph.D. degrees from Tsinghua University and Massachusetts Institute of Technology, respectively. His current research focuses on fundamental and applied aspects of light and materials interactions for advanced optoelectronic materials, devices, and systems with applications in energy and healthcare.

Ni Zhao is currently an associate professor in the Department of Electronic Engineering at the Chinese University of Hong Kong (CUHK). She received her bachelor and master degrees in materials science and engineering from Tsinghua University and McMaster University, respectively, and her Ph.D. degree in physics from the University of Cambridge. Her research interests include optoelectronic and bioelectronic devices based on organic and nanostructured materials, and characterizations of the electronic processes in these devices.

With further etching in HF solution, GaAs membranes are fully released, suspending in solvents. It is found that hydrochloric acid (HCl)-based solution is capable of undercutting AlAs sacrificial layers in GaAs-based devices, rendering a better compatibility with SiO_2- and Si_3N_4-based encapsulating

Table 1. Representative release methods to form single-crystalline thin-film membranes and devices based on group IV and III–V semiconductors.

Active layer	Sacrificial layer	Substrate	Release method	Reference
Si	SiO_2	Si	HF wet etch	[6,10]
Si{111}	–	Si{111}	KOH wet etch	[14,15]
Si	–	Si	Controlled spalling	[36,37]
Ge/SiGe	SiO_2	Si	HF wet etch	[11]
Ge	–	Ge	Controlled spalling	[37]
SiC	SiO_2	Si	HF wet etch	[13]
GaAs	–	GaAs	Controlled spalling	[37]
GaAs	Graphene	GaAs	Mechanical	[39]
GaAs/InGaP	AlAs	GaAs	HF/HCl wet etch	[17–22]
GaAs/InGaP	AlInP/InGaP	GaAs	HCl wet etch	[23,24,58]
InGaAs/InP	InGaAs/InAlAs	InP	$FeCl_3$ wet etch	[25–27]
InP	Graphene	InP	Mechanical	[39]
GaP	Graphene	GaP	Mechanical	[39]
GaN	Graphene	SiC	Mechanical	[40]
GaN	–	GaN	Controlled spalling	[38]
GaN	–	Sapphire	Laser liftoff	[29–31]
GaN	ZnO	Sapphire	HCl wet etch	[32,34]
GaN	BN	Sapphire	Mechanical	[33]
GaN	–	Si{111}	KOH wet etch	[16]
InAs	InGaSb	GaSb	NH_4OH wet etch	[28]

films.[22] One issue associated with AlAs sacrificial etching in HF solution is that certain reaction byproducts such as AlF_3, $AlF_n \cdot (H_2O)_{6-n}]^{(3-n)+}$, and Al_2O_3 are difficult to dissolve in the solution. An alternative approach is to implement phosphide-based material, such as aluminum indium phosphide (AlInP), which is lattice matched to GaAs as the sacrificial interlayer. AlInP, InGaP, and indium phosphide (InP) are known to dissolve quickly in the HCl-based solution while generating highly soluble etching byproducts ($AlCl_3$, $InCl_3$, and PH_3). After selective etching and epitaxial release, atomically smooth GaAs surfaces, which is ideal for III–V wafer recycling, can be obtained.[23,24] For indium gallium arsenide (InGaAs) and InP thin-film devices grown on InP, InGaAs and InAlAs can serve as an effective and lattice matched sacrificial layer, which can be selectively eliminated by iron chloride ($FeCl_3$) solutions to obtain freestanding InGaAs-based lasers and detectors.[25–27] Similarly, indium gallium antimonide (InGaSb), which can be etched away by ammonia (NH_4OH)-based solutions, is used as a sacrificial layer for indium arsenide (InAs) thin-film devices grown on the GaSb substrate, with high-performing InAs transistors demonstrated onto heterogeneous substrates.[28]

Other techniques, referred to as "physical" or "dry" process, have been proposed to release epitaxial thin-film devices from growth substrates without using solution-based chemical etching. For example, the laser liftoff technique[29–31] is introduced to release thin-film GaN/InGaN devices grown on sapphire substrates without the use of solution. With this technique, ultraviolet laser beam (for example, krypton fluoride KrF excimer laser at 248 nm) is applied to thermally decompose GaN into gallium (Ga) metal and nitrogen gas at the interface. To achieve epitaxial

liftoff effect, zinc oxide (ZnO) or boron nitride (BN) is used as interlayers between GaN-based devices and sapphire, and the devices are released via wet etching or mechanical separation.[32–34] Alternatively, controlled spalling technology (CST) is investigated as a "kerf-free" method to directly exfoliate thin-film semiconductor membranes and devices from substrates made of the same materials. It is based on a unique mechanical fracture mode where a surface layer with tensile stress induces cracks parallel to the thin-film/substrate interface.[35] Via CST, thin-film membranes, epitaxial layers, and fully formed devices can be formed from semiconductor wafers and even ingots, with substrates such as Si, Ge, GaAs, and GaN.[36–38] Recently, remote homoepitaxy is introduced to facilitate exfoliation, by which a monolayer graphene is applied on III–V growth substrates without disrupting the continuity of the lattice-matched epitaxial growth. The inserted graphene monolayer can significantly reduce the mechanical bonding between the epitaxially grown III–V layers and substrates, and thus resulting in easier exfoliation of thin-film devices. Such approach has been applied to GaAs-, InP-, GaP-, and GaN-based materials and relative thin-film devices such as LEDs, solar cells, etc.[39,40]

2.1.2. Organic Semiconductor Materials

Organic semiconductor materials, originally developed for optoelectronics such as organic light-emitting diode (OLED) and organic photovoltaics, have demonstrated great potential for biomedical applications.[41,42] **Figure 2** shows examples of organic photoactive materials, including both polymeric and small molecule, for flexible optoelectronics. It is worth noting that several review papers have provided comprehensive review on organic optoelectronics.[43–45] Here, we will specifically highlight the materials and the characteristic properties relevant to flexible biointegrated applications.

Although organic semiconductors are in general inferior to their inorganic counterparts in terms of electronic performance, the material family possesses certain unique properties that are complementary to those of inorganic semiconductors. The most advantageous attribute of all is their chemical versatility. Tuning optoelectronic properties is made easy as the molecular structure can be controlled by chemical synthesis with an aim to render high sensitivity to optical or electrical stimuli. In addition, organic semiconductors allow low-temperature processing techniques such as spin coating, thermal evaporation, and inkjet printing, promising low-cost and high-throughput devices readily fabricated on flexible substrates. Moreover, thanks to the weak van der Waals intermolecular interaction, the thin film of organic semiconductors possesses the ideal intrinsic mechanical flexibility for device integration. Lastly, the Young's modulus of organic materials is usually
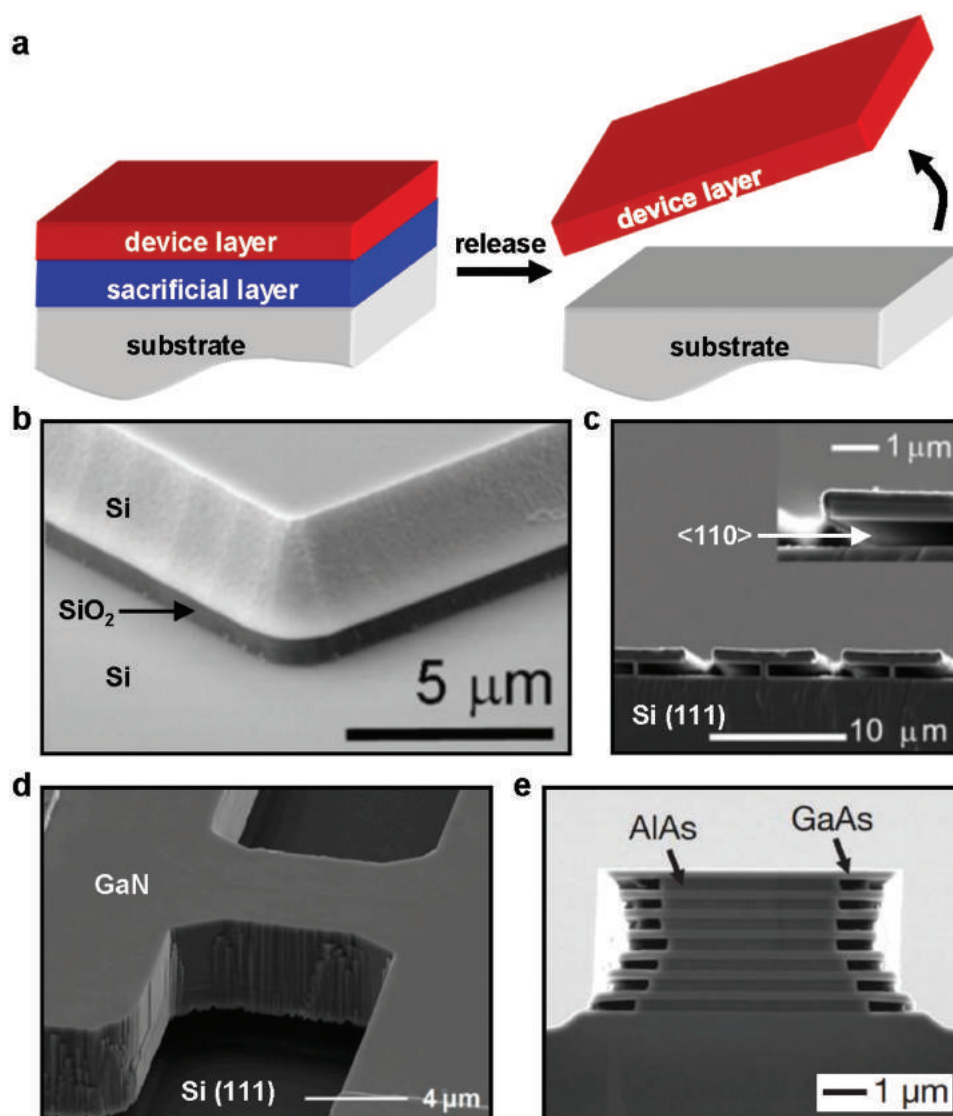
Figure 1. a) Schematic illustration of the release process to form thin-film semiconductor devices from original growth substrates. Scanning electron microscopy (SEM) images of different single-crystalline semiconductor thin films released from substrates: b) Si released from SOI substrates by undercut SiO_2. Reproduced with permission.[10] Copyright 2012, IOP Publishing; c) Si released from a Si(111) wafer by KOH anisotropic etching. Reproduced with permission.[15] Copyright 2007, Wiley-VCH; d) GaN released from a Si(111) wafer by KOH etching. Reproduced with permission.[16] Copyright 2011, National Academy of Sciences (NAS); e) GaAs membranes released from GaAs substrates by selective etching the AlAs sacrificial layers in between Reproduced with permission.[20] Copyright 2010, Nature Publishing Group.

much smaller than that of the inorganic semiconductors and more comparable with biotissues. Intrinsically stretchable organic semiconductor materials have been developed recently via novel molecular design[46,47] or polymer/polymer composite development.[48,49] Further details about stretchable organic semiconductors are discussed in Section 2.3.1.

2.2. Fabrication Processes

2.2.1. Inorganic Optoelectronic Devices

Based on the epitaxial release techniques reviewed in the previous section, thin-film microscale optoelectronic devices made by various single-crystalline inorganic semiconductors are formed and can be deterministically integrated with heterogeneous substrates via methods such as transfer printing.[6,50] The integration process is typically performed at room temperature or mildly elevated temperatures (<200 °C) which is suitable for both rigid substrates (Si, glasses, ceramics, etc.) and flexible sheets such as polyimide (PI), polyethylene terephthalate (PET), and polydimethylsiloxane (PDMS). Such heterogeneous or hybrid device architectures, i.e., inorganic/organic and rigid/flexible integration, are significant for biomedical uses. As opposed to conventional approach, it becomes feasible to achieve facile combination of different high-performance optoelectronic devices (Si, GaAs, Ge, GaN, etc.) within the same platform, offering tremendous possibilities for application in
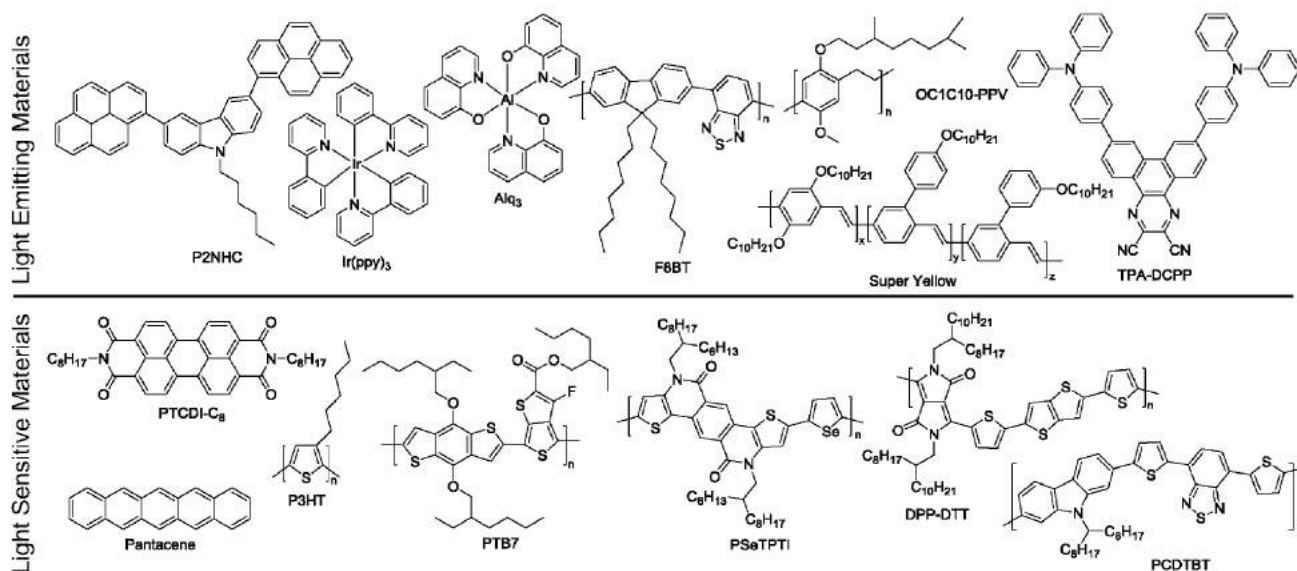
Figure 2. Molecular structures of common organic photoactive materials.

fields such as advanced displays, energy harvesting, and communication. Examples of these devices are as illustrated in **Figure 3**.

Thin-film (thickness < 10 μm), microscale (size < 50 μm) GaN-based blue LEDs and AlInGaP-based red LEDs are presented in Figure 3a,b, respectively.[31,51] Recently, similar assembling approaches are adopted to demonstrate red–green–blue (RGB) micro-LED arrays made by InGaN and AlInGaP devices with a size of 8 μm × 15 μm (Figure 3c).[52] Other advanced light

sources including thin-film edge and surface-emitting III–V lasers in near-infrared and communication bands (850 and 1550 nm, respectively) are demonstrated on Si and flexible substrates (Figure 3d), which opens way for practical applications for on-chip telecommunications and biological sensing.[22,53–56]

Printing-based approaches for various light receivers are also demonstrated. GaAs- and InGaP-based thin-film photovoltaic cells and photodetector arrays are fabricated on flexible substrates, with capabilities for solar energy harvesting and
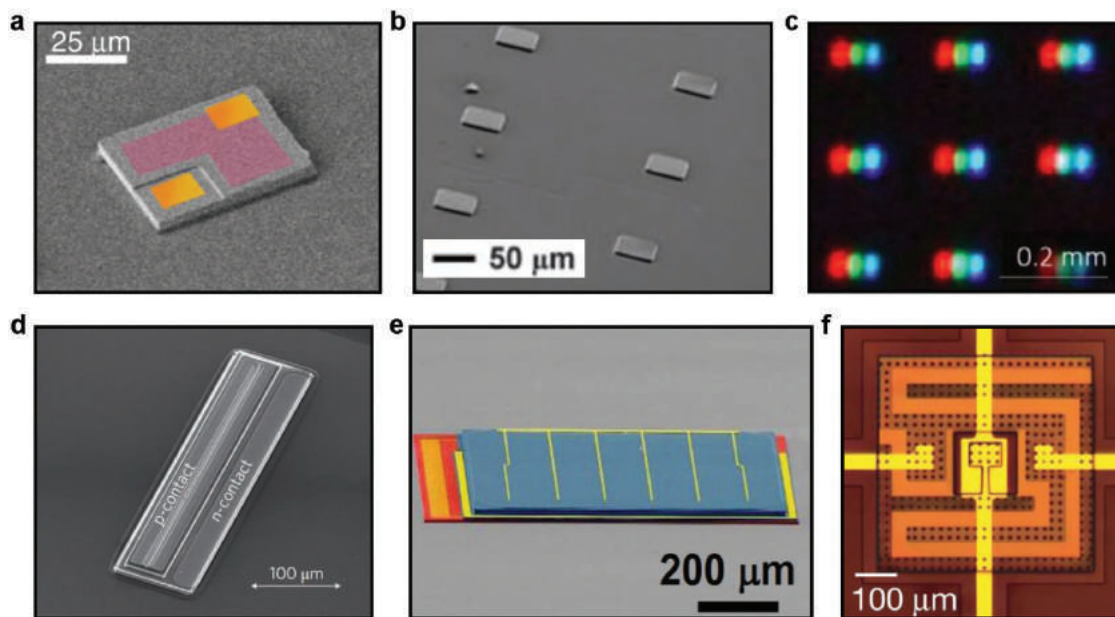
Figure 3. Representative microscale, thin-film optoelectronic devices transferred onto heterogeneous substrates. a) An InGaN blue LED. Reproduced with permission.[31] Copyright 2013, American Association for the Advancement of Science (AAAS); b) an AlInGaP red LED array. Reproduced with permission.[51] Copyright 2009, AAAS; c) a III–V-based RGB micro-LED array for displays. Reproduced with permission.[52] Copyright 2017, OSA Publishing; d) a GaAs-based edge-emitting laser. Reproduced with permission.[53] Copyright 2012, Nature Publishing Group; e) a four-junction InGaP/GaAs/InGaAsNSb//Ge solar cell by printing. Reproduced with permission.[58] Copyright 2014, Nature Publishing Group; f) a Si photodetector. Reproduced with permission.[60] Copyright 2008, Nature Publishing Group.

**ADVANCED
SCIENCE NEWS**

www.advancedsciencenews.com

**ADVANCED
MATERIALS**

www.advmat.de
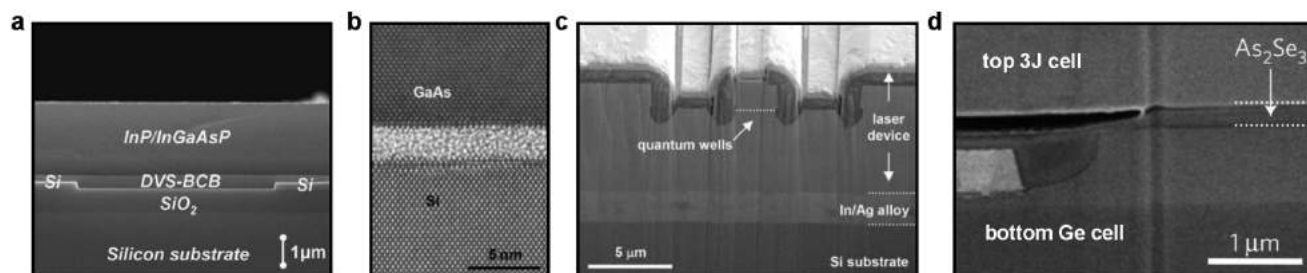
Figure 4. Cross-sectional electron microscopy images for thin-film semiconductor devices on heterogeneous substrates with different interfaces. a) InP/InGaAsP on Si with a divinylsiloxane-bis-benzocyclobutene (DVS-BCB) interface. Reproduced with permission.[62] Copyright 2007, Elsevier; b) GaAs on Si by direct fusion bonding, with amorphous SiO$_2$ in between. Reproduced with permission.[65] Copyright 2012, Nature Publishing Group; c) a GaAs laser on Si with an In/Ag-alloy-based interface. Reproduced with permission.[22] Copyright 2015, Wiley-VCH; d) a 3J InGaP/GaAs/InGaAsNSb solar cell on Ge with an As$_2$Se$_3$ interface. Reproduced with permission.[58] Copyright 2014, Nature Publishing Group.

infrared imaging.[20,21,57–59] Figure 3e illustrates a four-terminal, quadruple junction solar cell, consisting of InGaP/GaAs/InGaAsNSb top cells and a Ge bottom cell, created via epitaxial liftoff and stacking techniques.[58] Such multijunction solar cell addresses the drawbacks of the lattice match and current match associated with conventional growth methods, showing a combined 43.9% efficiency rate under concentration. Figure 3f gives an example of such method to form thin-film Si-based photodiodes and solar cells from SOI or Si{111} wafers.[6,14,60,61]

One of the unique advantages of heterogeneous integration of optoelectronic devices lies within the flexibility to choose the bonding interface according to the purpose of application. **Figure 4** shows several examples of optoelectronic devices transferred onto heterogeneous substrates using different interfacial materials as the device-substrate interface. A common approach is to select organic-based materials with reasonably good bonding strength, usually found in hydroxyl group, as the adhesive. The organic bonding layer can be achieved via solution-based methods and cured by thermal or light treatments to create relatively thick films (>100 nm) that is suitable for interface planarization and tolerable for surface roughness (Figure 4a). In principle, interfaces formed by organic materials, such as SU-8, polyimide, and benzocyclobutene (BCB),[62–64] are electrically and thermal insulating. In some cases, direct bonding is performed between two semiconductor layers to form electrically and thermally conductive interfaces (Figure 4b). In general, successful bonding requires extremely clean and smooth device surfaces specifically treated, followed by subsequent annealing.[65,66] In the case when direct bonding is not attainable and when organic adhesives fail to provide sufficient thermal conductance, metallic-based interfacial materials (usually with a low melting or eutectic point) can be employed to facilitate the bonding.[22,26] Figure 4c presents a GaAs thin-film laser printed onto Si substrates with an indium/silver (In/Ag)-based interface so as to reduce the device operation temperature under continuous current injection.[22] Optical coupling at interfaces is critical for solar cell structures. Recently, chalcogenide glass-based materials are selected to serve as interfaces for their properties of being electrically insulating and infrared transparent. Such interfaces with refractive indices matched with semiconductors minimize optical losses at the stacked solar cells. Figure 4d illustrates the arsenic selenide (As$_2$Se$_3$) interface inside the high efficiency stacked four-junction InGaP/GaAs/InGaAsNSb//Ge cell as described in Figure 3e.[58]
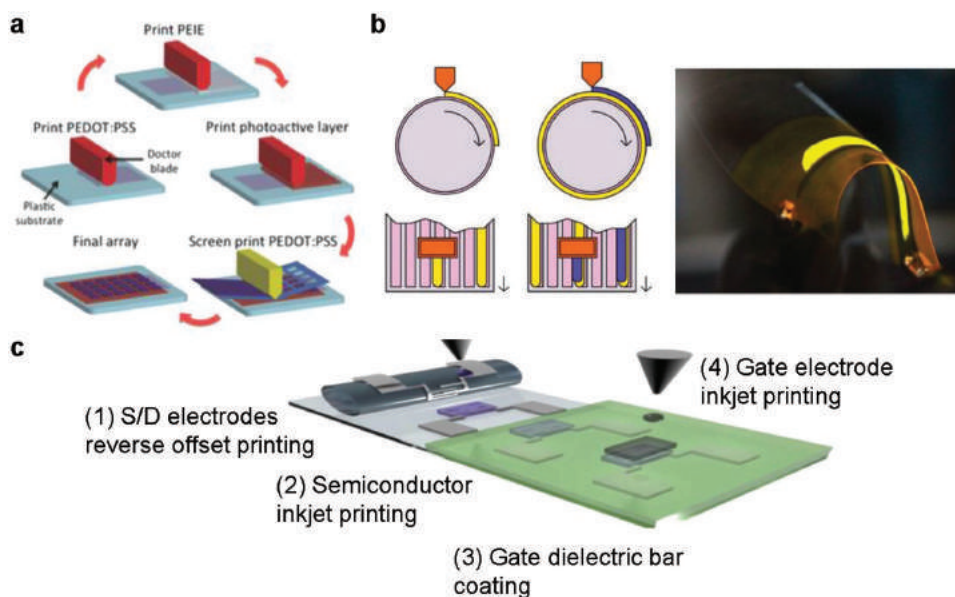
2.2.2. Organic Optoelectronic Devices

Unlike their inorganic counterparts, organic semiconductor materials can be deposited in a top-down manner through vacuum thermal evaporation or solution-based processes. Thermal evaporation is a favorable approach to form thin films of small molecules with high uniformity on flexible substrates including plastics, elastomers, and papers.[67–71] As demonstrated by Zhang et al., a flexible OFET-based memory structure was presented to obtain pentacene by thermal evaporation for selective solar-blind UV monitoring.[69] Solution-based processes, such as spin coating, blade coating, slot die, and inkjet printing, are commonly used for depositing polymeric materials.[72–80] By using blade coating, Pierre et al. demonstrated all-printed bulk heterojunction organic photodiodes (**Figure 5**a) with ≈3.45 × 10^{13} cm Hz$^{0.5}$ W$^{−1}$ detectivity, outperforming many inorganic photodiodes.[72] Sandström et al. introduced slot-die coating of large area light-emitting electrochemical cells on a PET substrate (Figure 5b) and achieved strong light emission from the cells with low operating voltages.[75] On the other hand, Kim et al. fabricated a device that yields highly sensitive organic phototransistor (OPT) arrays on a flexible PI substrate by combining inkjet printing and offset printing (Figure 5c).[80]

2.3. Device Design

2.3.1. Mechanical Design for Flexibility and Stretchability

To make a device or system flexible or stretchable, approximately five mechanical design strategies can be employed individually or in combination: 1) develop intrinsically flexible or stretchable active materials, 2) reduce device thickness, 3) locate active elements at a neutral mechanical plane, 4) create buckling or wavy-structured flexible devices, and 5) connect rigid device islands with flexible or stretchable interconnects.

Develop Intrinsically Flexible/Stretchable Active Materials: Stretchable conductors and semiconductors have been fabricated by using organic or composite-based materials. Typically, stretchable electrodes are made by dispersing a deformable conductive network in a stretchable material matrix. Liang et al. demonstrated a transparent composite electrode consisting of a thin silver nanowire (AgNW) network embedded in the surface layer of a rubbery poly(urethane acrylate) matrix.[81] The

**ADVANCED
SCIENCE NEWS**
www.advancedsciencenews.com

**ADVANCED
MATERIALS**
www.advmat.de

Figure 5. Examples of solution-based processes for organic optoelectronic devices. a) Fabrication process of all-printed OPDs. Reproduced with permission.[72] Copyright 2015, Wiley-VCH. b) Left: Schematic view of the slot-die of the active layer (yellow) and the anode (blue) of an light-emitting electrochemical cell (LEC); Right: Photograph of a slot-die-coated flexible LEC. Reproduced with permission.[75] Copyright 2012, Nature Publishing Group. c) Schematic process flow for the fabrication of OPTs based on a combination of various printing methods. Reproduced with permission.[80] Copyright 2014, Elsevier B.V.

polymer light-emitting diode (PLED) fabricated based on this composite electrode was capable of emitting light at a strain rate as high as 120% and even showed significantly improved efficiency in the stretched state. Recently, intrinsically stretchable organic semiconductor materials have also been developed. Bao et al. exploited the nanoconfinement effect of conjugated polymers inside of a soft and deformable elastomer to achieve stretchability.[49] In their design, charge transport occurs within the interconnected nanofibril aggregates of a high-mobility conjugated polymer (poly(2,5-bis(2-octyldodecyl)-3,6-di(thiophen-2yl)diketopyrolo[3,4-c]pyrrole-1,4-dione-alt-thieno[3,2-b]thiophen (DPPT-TT)), while deformation-induced crack propagation can be effectively prevented by uniformly wrapping DPPT-TT nanofibers with a soft elastomer based on polystyrene-*block*-poly(ethylene-*ran*-butylene)-*block*-polystyrene. The composite semiconductor film can be stretched to 100% strain rate while maintaining high mobility. Oh et al. developed stretchable semiconducting polymers by introducing 2,6-pyridine dicarboxamide moieties in conjugated polymer backbones to create hydrogen bonding units (**Figure 6**a, bottom).[47] Organic transistors fabricated from the stretchable semiconducting polymers exhibited a mobility as high as 1.3 cm^2 V^{-1} s^{-1} and a high on/off ratio over 10^6. The transistors can be strained up to 100% with a slow linear decrease in mobility. After releasing the strain, the mobility resumes nearly to the prestrain value.

Reduce Device Thickness: As a principle, bending-induced strain decreases linearly with respect to material thickness. It has been demonstrated that silicon wafers become highly flexible when the thickness is reduced to nanoscale.[82] For organic electronics, ultrathin device structure plays a critical role in enhancing flexibility and bendability. Figure 6b shows a sub-2 µm thick organic solar cell wrapped around a human hair with a radius of 35 µm, demonstrating the remarkable bending

flexibility of the device.[83] Ultrathin organic electronics can be achieved by fabricating devices directly on thin polymeric substrates or by peeling off the devices fabricated on rigid substrate first covered with a thin relief layer.[84,85]

Use Neutral Mechanical Plane: In this approach, the active device layers are located at the neutral mechanical plane (NMP)[86] where the compressive and tensile strains induced by bending are minimized. For instance, Someya and co-workers sandwiched organic transistors between a 13 µm thick polyimide substrate and a parylene/Au/parylene encapsulation stack of the same thickness (e.g., ≈13 µm). Within such layout the ≈106 nm thin transistors are positioned approximately at the NMP, and they exhibited stable performance even when bent to a radius of 100 µm.[87] Similar concept has been applied to enable ultraflexible PLEDs (Figure 6c).[88]

Create Buckling: The formation of periodic buckling is achieved by attaching a flexible and thin device to a prestretched elastomeric substrate followed by releasing the entire structure (Figure 6d). As such, the device is stretched to the prestrain status. In principle, this approach can make any flexible electronic devices stretchable. Deterministic in-plane and out-of-plane buckling (Figure 6e) structures have been demonstrated for inorganic electronic devices.[51,59,60,89] The buckling strategy has also been used in combination with thickness reduction and/or NMP approaches to achieve stretchable PLEDs, photovoltaic devices, and transistors, which can be stretched up to 100% of their original sizes while the performance is only slightly affected.[83,88,90,91]

Connect Rigid Islands with Flexible/Stretchable Interconnects: Microscale, thin-film devices transferred onto flexible and stretchable substrates are interconnected to form functional circuit systems. Flexibility of integrated device arrays is achieved by the reduced flexural rigidity associated with the

**ADVANCED
SCIENCE NEWS**

www.advancedsciencenews.com

**ADVANCED
MATERIALS**

www.advmat.de
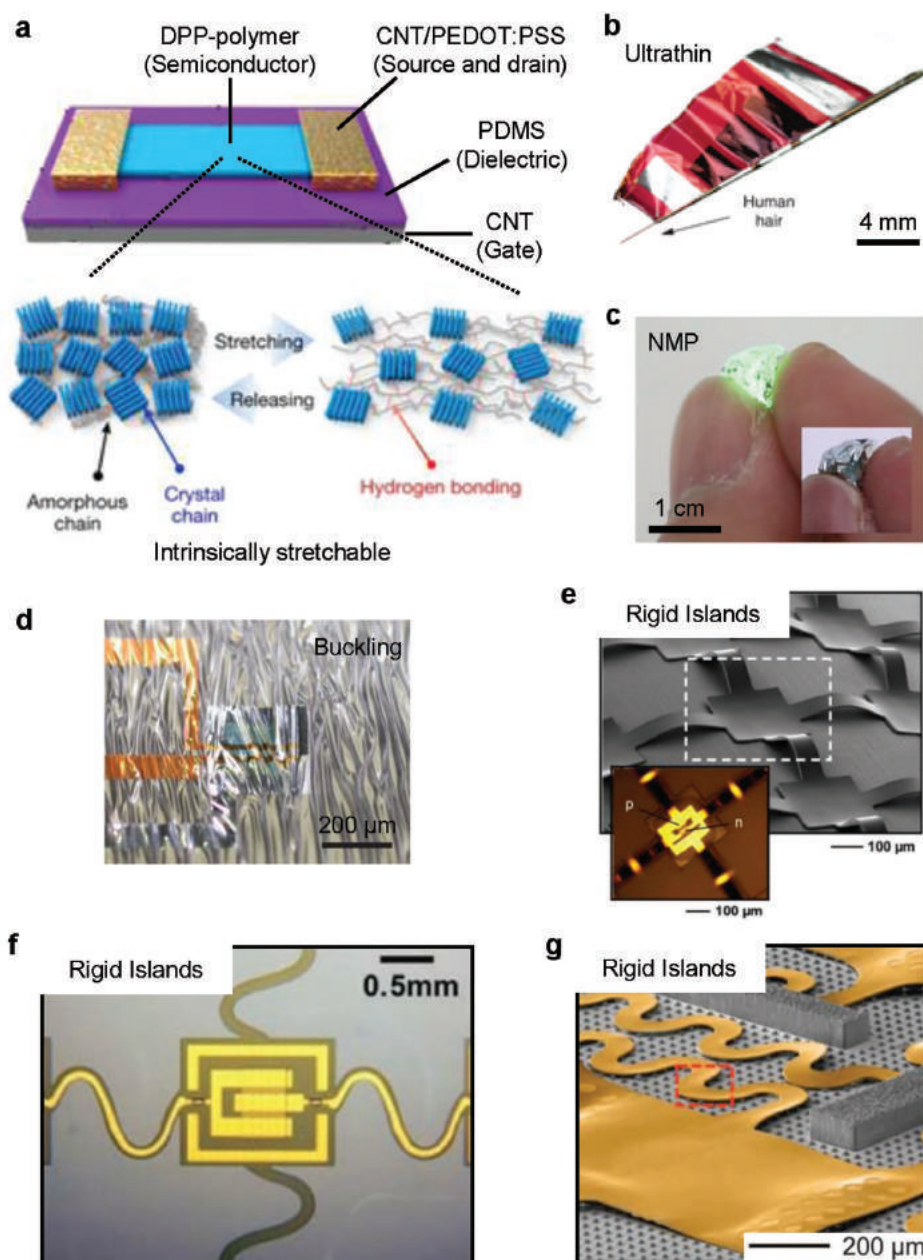
Figure 6. Examples of flexible/stretchable electronics using different strategies. a) Intrinsically stretchable-material-based devices. Reproduced with permission.[47] Copyright 2016, Nature Publishing Group. b) Ultrathin devices. Reproduced with permission.[83] Copyright 2012, Nature Publishing Group. c) Neutral mechanical plane. Reproduced with permission.[88] Copyright 2016, AAAS. d) Buckling. Reproduced with permission.[91] Copyright 2013, Nature Publishing Group. e–g) Rigid islands: e) Stretchable AlInGaP red LEDs interconnected by outplane buckled mesh electrodes on a PDMS substrate. Reproduced with permission.[51] Copyright 2009, AAAS; f) A Si diode within flexible circuits with serpentine metallization. Reproduced with permission.[63] Copyright 2011, AAAS; g) thin-film stretchable serpentine circuits floating in soft microfluidics. Reproduced with permission.[93] Copyright 2014, AAAS.

thin-film geometry of inorganic semiconductor membranes, as well as the mechanical design of the neutral plane.[4,63,92] Furthermore, system stretchability is accomplished by advanced mechanical design strategies,[5] including creating deterministic in-plane and out-plane buckling (Figure 6e),[51,59,60,89] nonuniformly distributing stress onto "soft" organic and metallic regions (Figure 6f),[63] and suspending devices and circuits in fluids (Figure 6g).[93] Novel designs of stretchable

electrical interconnects also contribute to the improvement of system stretchability. Conductive filler-based elastic conductors, e.g., carbon nanotubes and conductive polymers, have been developed to connect rigid electronic islands.[94–96] The buckled, arc-shaped "ribbon cables" of metal have been designed to accommodate applied strains of 100% or more.[97,98] This method allows transforming rigid devices to stretchable system while the high performance is maintained.

**ADVANCED
SCIENCE NEWS**

www.advancedsciencenews.com

**ADVANCED
MATERIALS**

www.advmat.de

Table 2. Properties of typical substrates and encapsulation layers.

Layer	Material	Young's modulus [GPa]	Thermal stability [°C]	Chemical resistance	Moisture and oxygen permeability
Substrate	PI	≈8	<450 °C	Weak acids and alkalis, alcohols, and acetone	Allow for moisture absorption and oxygen permeability
	PEN	5	<180 °C	Weak acids and alkalis, alcohols	Easily permeated by water and oxygen
	PET	4	<130 °C	Dissolvable in acetone	Low permeability to moisture and oxygen
	Parylene C	2.8	<125 °C	Acids, alkalis, and solvents	Low permeability to moisture and oxygen
Encapsulation	PDMS	$(0.36–0.87) \times 10^{-3}$	<279 °C	Excellent barrier to biofluids and tissues	Permeated by water vapor and oxygen
	Organic/inorganic multilayer	–	<300 °C	Good barrier to fluids	Decent impermeability
	Thermally SiO_2	66.3–74.8	>1000 °C	Excellent barrier to biofluids	Impermeability to water

2.3.2. Materials for Substrate, Encapsulation, and Adhesion

Substrate: Substrate provides mechanical support for the fabrication and operation of flexible electronic and optoelectronic devices, and affects device properties. Major factors to be considered when selecting substrate material for biointegrated applications include flexibility, transparency, thermal stability, chemical resistance, and biocompatibility. Typically, plastic polymers and elastomers are selected for flexible electronics. The chemical and physical properties of typical substrate and encapsulation materials are summarized in **Table 2**.

Among all polymer substrates, polyimide is considered to be compatible with almost all fabrication processes for organic electronic devices thanks to its great mechanical flexibility, thermal stability, chemical resistance,[99,100] and biocompatibility. Besides the commercially available PI films, ultrathin and smooth PI layers with micrometer to sub-micrometer thickness can be formed via solution-based processes such as spin coating. As the optical absorption onset or the regular PI materials is around 400–500 nm, their applications in the ultraviolet-to-blue range is limited. Recently, transparent PI substrates have been developed through prepolymer structure design, such as polymerization of poly(amic acid)-containing trifluoromethyl (−CF3), sulfone (−SO2), or ether (−O−) group.[101,102] Poly(ethylene terephthalate) and polyethylene naphthalate (PEN) films have been widely used for flexible organic optoelectronics due to their commercial availability, high transparency in the visible wavelength region, as well as the capability to serve as barrier against gas, moisture, or even alcohol. Ultrathin PET/PEN (1.4 µm) can be adhered to polydimethylsiloxane-coated rigid substrates via van der Waals bonding, thereby allowing standard laboratory device fabrication processes prior to the liftoff of the device from the rigid substrates.[102] However, the thermal stability of PET and PEN is lower than that of PI, and PET can be partially dissolved by some organic solvents such as acetone. Parylene C has been used as flexible substrate and protective layer of devices for in vivo applications owning to its extremely low permeability to gas, moisture, chemicals, and other corrosive molecules, as well as high electrical resistivity. Parylene is Food and Drug Administration approved material for implantable devices such as pacemaker.[103] Parylene C film is usually formed through chemical vapor deposition. By carefully controlling the deposition parameters, micrometer-thick, pinhole-free parylene films can be achieved.

Elastomeric rubber-like materials, such as PDMS, Ecoflex, and polyurethane (PU), have been used as substrates to yield not only flexible but also stretchable devices. PDMS has been the dominant material for stretchable electronics due to its intrinsic stretchability, optical transparency, chemical inertness, thermal stability, variable mechanical properties, and biocompatibility. The surface of PDMS can easily be modified from hydrophobic to hydrophilic by surface treatment, such as oxygen plasma, ultraviolet/ozone, and chemical functionalization.[104,105]

Figure 7a–g shows examples of inorganic optoelectronic device arrays on flexible and stretchable substrates. Arrays of InGaN blue LEDs (Figure 7a),[16,30] AlGaInP red LEDs (Figure 7b),[51,89] and combined RGB micro-LEDs (Figure 7c) are formed onto heterogeneous substrates, such as PET, PDMS, and glass, to develop deformable, semitransparent, monochromatic, and polychromatic displays.[52] Similar concepts are adopted for light receivers and waveguides to realize inorganic material (Si, III–V, glass, etc.) based solar cells (Figure 7d),[14,59] photodetectors (Figure 7e),[60,98] phototransistors (Figure 7f),[106] waveguides and resonators (Figure 7g)[92,107] on flexible and even highly curved and stretchable substrates. As a result, further progress has been made in areas such as power supply, imaging, and sensing. Organic electronics has also been fabricated on flexible substrates such as PI, PET, and parylene.[83,99,103]

Encapsulation: Apart from mechanical flexibility, the stability and controllability of a biointegrated optoelectronic device is essential for operation under extreme circumstances such as prolonged immersion in biofluids. To accommodate different biomedical and clinical applications, encapsulation strategies are implemented, ranging from long-live moisture barriers to fully degradable device platforms in biosystems, as described in **Figure 8**. In many cases, organic-based thin-film layers (SU8, PDMS) are used as device encapsulants (Figure 8a,b) so as to ensure the system stretchability and the protection of electronic devices from water. Implanted blue and red micro-LED arrays encapsulated by SU8 and PDMS coatings are proven to be operable in living animals for months;[89,108] however, organic materials are inevitably water permeable after longtime immersion which leads to eventual electronic failure. By reducing pinholes,

**ADVANCED
SCIENCE NEWS**

www.advancedsciencenews.com

**ADVANCED
MATERIALS**

www.advmat.de
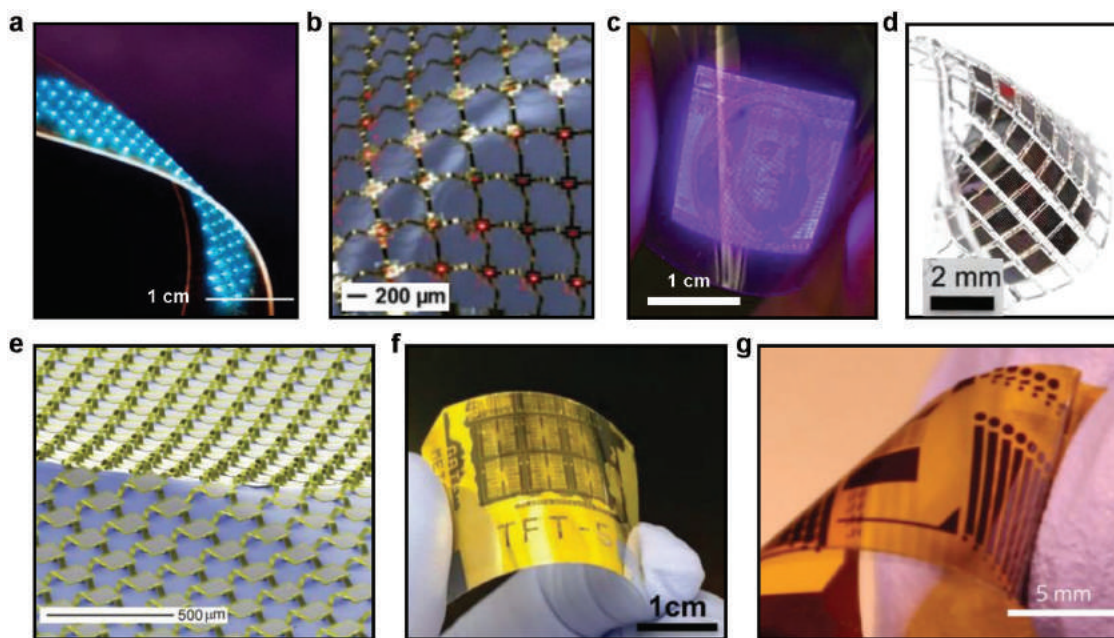
Figure 7. Optical microscopy and SEM images of representative thin-film optoelectronic devices and interconnected array systems formed on flexible and stretchable substrates. a) An InGaN blue LED array interconnected on a bent substrate. Reproduced with permission.[16] Copyright 2011, NAS. b) A stretchable AlInGaP red LED array on PDMS. Reproduced with permission.[51] Copyright 2009, AAAS. c) A flexible RGB display based on III–V micro-LED arrays. Reproduced with permission.[52] Copyright 2017, OSA Publishing. d) Stretchable GaAs microscale solar cells on PDMS. Reproduced with permission.[59] Copyright 2011, Wiley-VCH. e) Arrays of thin Si photodetectors with outplane buckling interconnected metal grids on a curvilinear substrate. Reproduced with permission.[98] Copyright 2009, Wiley-VCH. f) Arrays of Si phototransistors on a flexible substrate. Reproduced with permission.[106] Copyright 2016, Wiley-VCH. g) Flexible arrays of chalcogenide-glass-based mid-IR waveguides and resonators. Reproduced with permission.[92] Copyright 2014, Nature Publishing Group.

the protectiveness of organic/inorganic multilayer coatings can be improved, yet still not moisture-impermeable enough.[109] Recently, a unique encapsulation approach based on defect-free, thermal SiO_2 is proposed.[110] The high-quality SiO_2 layer is thermally grown on crystalline Si wafers and then transferred onto flexible substrates with functional devices while the Si wafer is completely eliminated afterward (Figure 8c). Such an ultrathin SiO_2 layer (≈100 nm) exhibits outstanding moisture impermeability and acts as a nearly perfect water barrier for a great span of time (up to several decades) in biofluids (Figure 8d). The degradation rate is less than 0.01 nm per day in phosphate-buffered saline (PBS) solution (pH = 7.4) at room temperature (25 °C). Accelerated dissolution tests show that the hydrolysis of the thermal SiO_2 layer generates a defect-free surface (Figure 8d) with much lower electronic leakage than other oxides created at lower temperatures, such as SiO_2 by plasma-enhanced chemical vapor deposition and Al_2O_3 by atomic layer deposition (Figure 8e).

Alternatively, certain implantable devices do not need to be in operation permanently and are to be removed after certain clinical practices. Under these circumstances, biointegrated electronic and optical devices that dissolve naturally in physiological conditions have received much attention[111] since potential risk of surgical complications can be avoided. Comprising solely of biodegradable active materials (metals,[112] semiconductors,[113,114] and dielectrics[115]) and encapsulants,[116] implantable optoelectronic devices consisted of photonic crystals,[117] photodetectors,[111] solar cells,[113] waveguides,[118–120]

and light emitters[121,122] can dissolve in biological environments in a controlled manner after use (Figure 8f).

Adhesion between the Device and Biotissue: In certain biointegrated applications, epidermal or implantable devices need to establish intimate and conformal contact with the surface of the tissue. Nevertheless, the mismatch of the mechanical properties between the tissue and device is almost inevitable. For instance, the Young's modulus (*E*) of PI films is ≈8 GPa, while the *E* values of human skin and brain are only 140–600 and 1 kPa, respectively. One way to address the problem is to implement highly stretchable mechanical components (such as serpentine interconnects) within an ultrathin device. In such a manner, the device adheres directly to the surface of the tissue through van der Waals forces alone, without the use of mechanical fixturing, hardware, or adhesive tapes.[123,124] Another strategy to ensure conformal contact is to use biocompatible gel-like adhesive with low Young's modulus to bond the device and tissue. Biomedical adhesives have been used for years in clinical applications. Recently, a type of commercially available medical-grade acrylic adhesive film has been used to achieve solid and seamless adhesion between flexible sensors and the skin. Such adhesive does not induce chemical or physical irritation while performing well even in areas of excessive hair or sweat.[125] Other advanced adhesive materials have been investigated with an aim to improve the adhesive strength, reusability, softness, and biodegradability. Examples of such adhesives include poly(vinyl alcohol)-containing polyrotaxane gel,[126] cross-linkable 3,4-dihydroxy-L-phenylalanie

ADVANCED
SCIENCE NEWS

www.advancedsciencenews.com

ADVANCED
MATERIALS

www.advmat.de
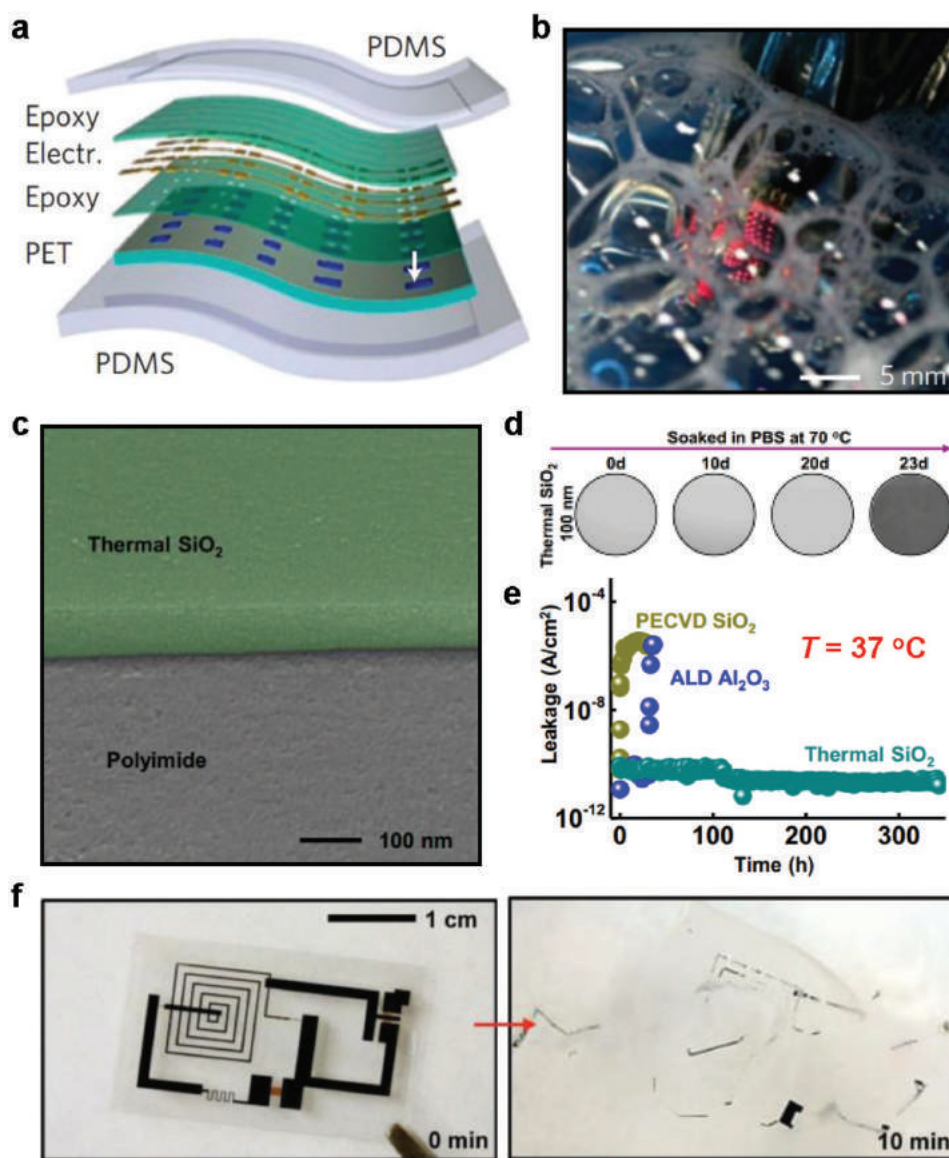
Figure 8. a) Schematic illustration of a flexible AlInGaP red LED array encapsulated by epoxy and PDMS. b) Operation of the encapsulated LED array immersed in soapy water. c) SEM image of a thermal SiO_2 thin film transferred onto polyimide. d) Optical images of a Mg surface encapsulated by thin-film thermal SiO_2 soaked in PBS solution at 70 °C for various numbers of days. e) Measured leakage currents for SiO_2 layers (100 nm thick) formed by different methods by soaking in PBS at 37 °C for various times. f) Images showing a physically transient circuit made of degradable electrodes, semiconductors, and substrates dissolved in water. a,b) Reproduced with permission.[89] Copyright 2010, Nature Publishing Group. c–e) Reproduced with permission.[110] Copyright 2016, NAS. f) Reproduced with permission.[111] Copyright 2012, AAAS.

(DOPA)-containing terpolymer adhesives,[127] modified PDMS-based elastomer,[10] and polymer/hydrogel composites.[128]

3. Biomedical Applications

In the previous section, we discuss the design and fabrication strategies for thin-film semiconductor materials and interfaces with unique electrical, optical, mechanical, and thermal properties. It is demonstrated that heterogeneously integrated devices exhibit superior performance than conventional optoelectronic devices. Additionally, fully assembled circuits and systems open

up opportunities in biomedical applications ranging from bio/chemical sensing, stimulation, imaging, to clinical pathology, diagnosis, and therapy. In this section, we provide examples of advanced optoelectronic devices and their applications in the development of biomimetic, epidermal, and implantable systems and biophotonic chips.

3.1. Biomimetic Systems

As devices with high-performing photon detection, modulation and emission capabilities are successfully formed onto

**ADVANCED
SCIENCE NEWS**

www.advancedsciencenews.com

**ADVANCED
MATERIALS**

www.advmat.de
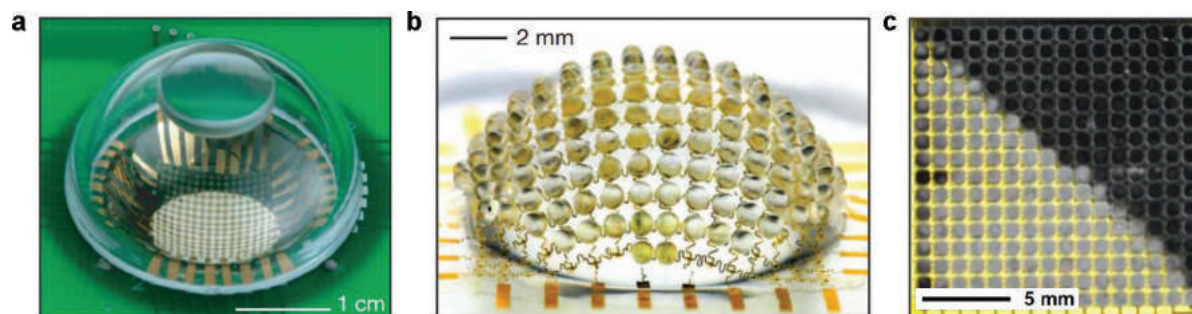
Figure 9. Photographs of representative biomimetic photonic systems based on flexible Si photodetector arrays. a) Hemispherical electronic eye cameras imitating the human eye. Reproduced with permission.[60] Copyright 2008 Nature Publishing Group. b) The arthropod compound eye structure. Reproduced with permission.[130] Copyright 2013, Nature Publishing Group. c) An adaptive camouflage electronic skin inspired by cephalopods. Reproduced with permission.[141] Copyright 2014, NAS.

flexible and stretchable substrates, there will be possibilities to develop advanced optoelectronic platforms that imitate the various structures and functions of the biological system. As shown in **Figure 9**a, thin-film, single-crystalline Si-based photodiode arrays transferred onto compressible elastomeric substrates form a hemispherical camera that is comparable to the human eye.[60] Such an electronic eye camera is not burdened with the complexity of multilens systems consisted of planar imaging sensors as conventional digital cameras. With a simple imaging lens, it achieves a wide viewing angle with low aberrations. With further implementation of dynamically deformable lenses and substrates, the electronic eye camera system will be provided with tunable zooming capability.[129] The hemispherical Si detector arrays integrated with convex microlenses on individual diodes are of similar design that mimics the arthropod compound eye with an acceptance angle near 180° (Figure 9b).[130] More recently, origami approaches have been reported for fabricating single−crystalline Si and MoS₂–graphene−based curved focal plane arrays and artificial compound eye structures, showing promise for future retinal prostheses.[131,132]

Organic photosensors have also been investigated for applications in visual prosthesis.[133,134] **Figure 10**a shows an organic photodetector focal plane arrays (FPA) on top of a plastic hemisphere with a radius of 1.0 cm that mimics the size, function, and architecture of the human eye.[133] The imaging capabilities of the FPA are demonstrated by its capability to generate a 7-bit gray scale image. In human retina, photoreceptor cells distinguish photons of different wavelengths and convert them into electronic signals in order to construct images. To mimic such a system and further extend the spectral range, Wang et al. demonstrated a retina-like organic photosensor structure with color-distinguishing and memory functions, as shown in Figure 10c–f.[135,136] Here, a voltage driver was used for photosensing while a floating-gate organic field-effect transistor was used for data readout. An ultrathin (800 nm) pixelated sensor array was made to conform the eyeball of a husky plush toy (Figure 10e), which sensed spatial resolved light excitation, mimicking the mammalian imaging process.

Recently, attention has been drawn to the development of artificial systems that simulate the optical, electrical, chemical, and mechanical properties of skins of various organisms.[63,128,137–139] In particular, man-made adaptive camouflage

skins inspired by cephalopods has been highly sought after.[140] As shown in Figure 9c, the solution is to laminate thin-film Si detector arrays along with thermally tunable and color-changing materials on a flexible thin sheet.[141] In this system, Si photodetectors receive light signals from the ambient environment and then provide feedback to change the colors of pixilated dyes by heating, thus imitating the surrounding areas. Incorporating different thermochromic dyes into the substrate can display polychromatic patterns.[142] By following the same principle, nonsilicon biomimetic device with materials of different spectral ranges can be applied to many domains such as UV and IR imaging and emitting systems.[61,143]

3.2. Epidermal Sensors

Advanced miniaturized optoelectronic devices, when integrated with flexible and stretchable substrates with mechanical properties similar to those of human skin, can be attached conformally to the epidermis to perform various sensing functionalities.[58,63,88,144] Compared to electronic sensors, biointegrated optoelectronic devices utilize optical signals to interact with biological systems with unique features such as high temporal/spatial/spectral resolutions, deep tissue penetration, and wireless energy/signal transmission. **Figure 11** illustrates several applications of optoelectronic epidermal sensors in the healthcare scenario.

In order to characterize skin conditions wirelessly, multiple photodetectors and LEDs of different colors are transferred onto flexible tapes and interconnected with external circuits to form a battery-free and stretchable photonic system.[145] Here, red and IR LEDs transmit optical signals to penetrate the skin, with transmission responses measured by an adjacent photodiode to determine the tissue oxygenation level in real time according to the difference of spectral responses between oxygenated and deoxygenated hemoglobin (Figure 11a). The devices are powered by and communicated with a smartphone with near-field communication chip coupled to an inductive coil. The results of temporal hemoglobin variation are compared against those collected by a commercially available wired oximeter (Figure 11b). To characterize UV dosage, similar device architecture is adopted, i.e., incorporating UV responsive dyes into flexible supporting substrate (Figure 11c). Since the dye is UV

**ADVANCED
SCIENCE NEWS**
www.advancedsciencenews.com

**ADVANCED
MATERIALS**
www.advmat.de
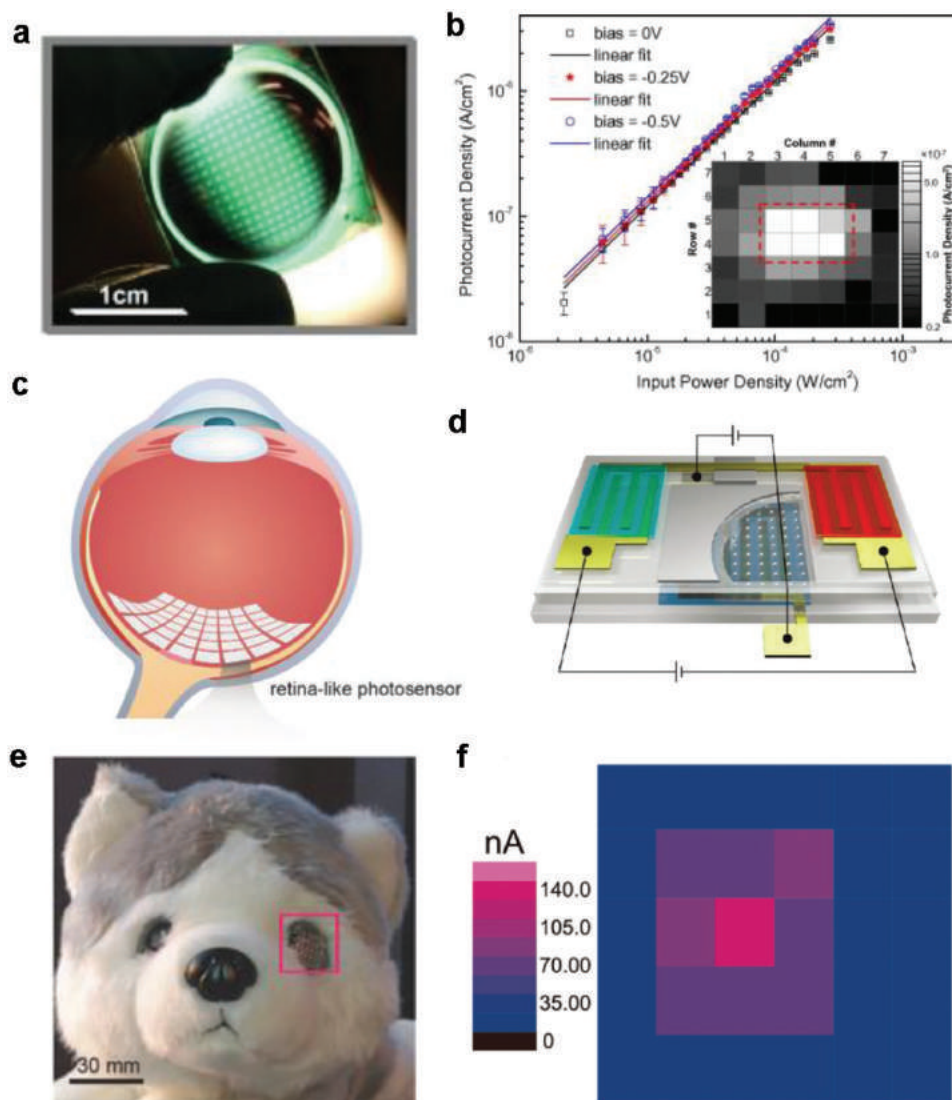
Figure 10. Organic biomimetic optoelectronic devices. a,b) Hemispherical electronic eye camera. Reproduced with permission.[133] Copyright 2008, Elsevier B.V. c–f) Retina-like dual-band organic photosensor array. Reproduced with permission.[136] Copyright 2017, Wiley-VCH.

bleachable, the optical transparency of the substrate varies under UV radiation and can be probed by photodiode receiving light signals from the IR and red LEDs (Figure 11d). Additional feature of this wireless optoelectronic platform is its capability to measure arterial pressures, heart rates, and skin colors.

The application of organic optoelectronic sensors for cardio-vascular monitoring has also been explored. Recently, further application in biomedical field has demonstrated promising results. Arias and co-workers demonstrated an all-organic flexible pulse oximeter based on green and red OLEDs paired with an organic photodiode (OPD),[146] and the results for pulse rate and oxygenation are with only 1% and 2% of errors, respectively. Samuel and co-workers showed that OLEDs and OPDs can be made flexible to improve the accuracy of the results, e.g., to better track muscle movement and tissue oxygenation (**Figure 12**).[147] In their study, the muscle contraction sensor consisting of four photodiodes surrounding one center-located light source (Figure 12a,b) is capable of measuring and

distinguishing the isometric and isotonic muscle contractions so as to control the movement of a robotic arm. To alleviate the stress and discomfort associated with epidermal sensors, Someya and co-workers developed an ultraflexible wearable device with three-color OLEDs and OPDs to track and display pulse, blood oxygen level, and other information on human skin (Figure 12e–g).[88]

To optimize the system performance, we combine the organic and inorganic devices in a hybrid sensing platform. As shown in **Figure 13**, we have developed epidermal and flexible near-infrared photoplethylsmogram (PPG) sensors by integrating a low-power, high-sensitivity organic BHJ pho-totransistor (OPT) with a high-efficiency inorganic LED.[148] While operating at a very low voltage (<3 V), the OPT still has an NIR responsivity as high as 3.5×10^5 A W^{-1} and NEP of 1.2×10^{-15} W Hz$^{-1/2}$, outperforming existing commercially available silicon photodiodes. Our PPG sensors are capable of continuously monitoring heart rate variability and precisely

**ADVANCED
SCIENCE NEWS**

www.advancedsciencenews.com

**ADVANCED
MATERIALS**

www.advmat.de
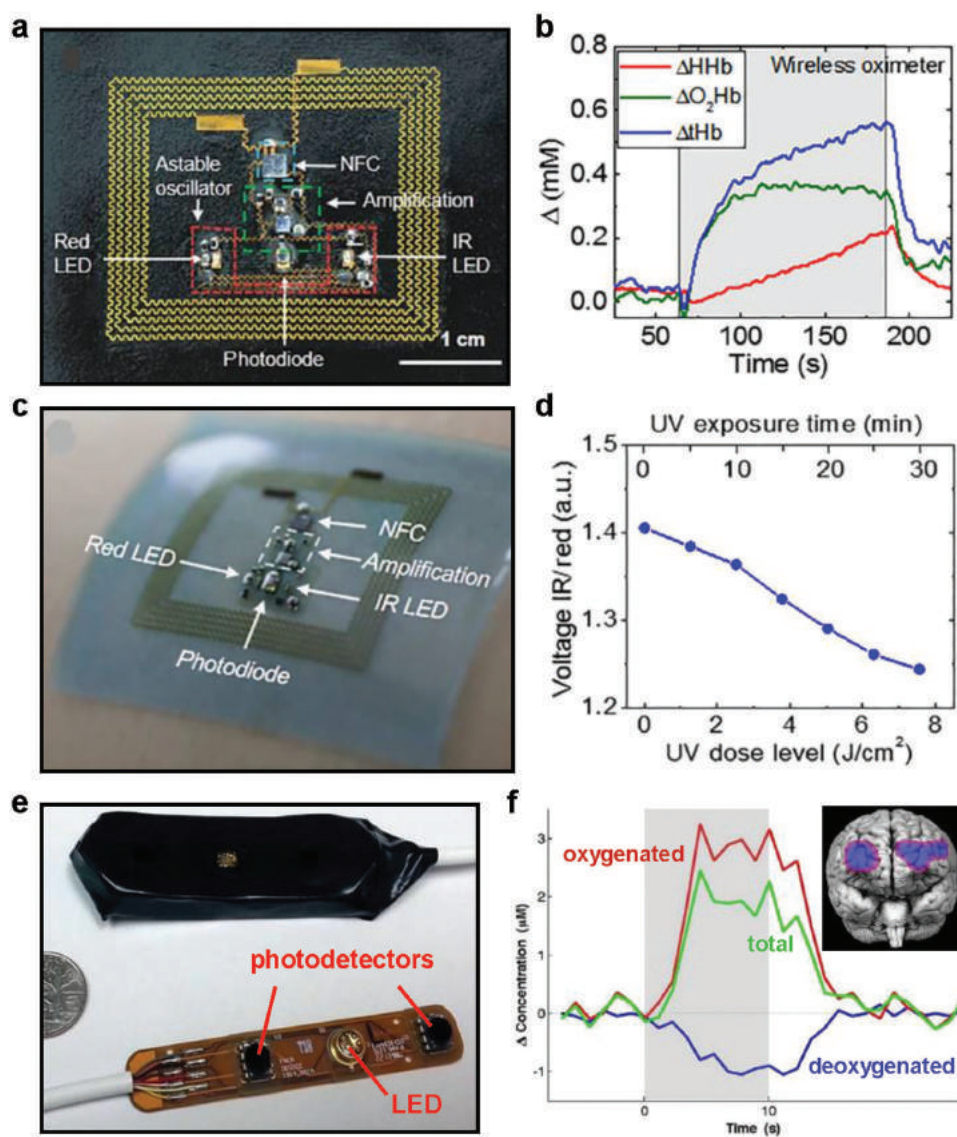
Figure 11. Representative skin-mounted optoelectronic systems. a) A stretchable epidermal wireless oximeter based on LEDs, photodetectors, and other circuit components integrated on a soft textile substrate. b) Recorded variations in the concentrations of deoxyhemoglobin (ΔHHb), oxyhemoglobin (ΔO$_2$Hb), and the total hemoglobin (ΔtHb) on the forearm. c) A epidermal UV dosimeter based on LEDs, photodetectors, and other circuit components integrated on a flexible substrate with UV sensitive dyes. d) Measured signals related to the UV exposure time and dose level. e) A miniaturized, head-mounted flexible fNIRS sensor pad with IR LEDs and photodiodes. f) Recorded variations in the concentrations of oxygenated, deoxygenated, and total hemoglobin under typical cortical activation (shadowed region). Inset: A typical fNIRS mapping. a–d) Reproduced with permission.[145] Copyright 2016, AAAS. e,f) Inset: Reproduced under the terms of CC-BY License.[149] Copyright 2015, The Authors, Published by Frontiers. f) Reproduced with permission.[150] Copyright 2012, Elsevier.

tracking the change of pulse pressure (PP) at different body positions, which is more reliable and energy efficient than conventional PPG sensors.

Functional near-infrared spectroscopy (fNIRS), the use of noninvasive technology examining oxygenation levels in cerebral cortex, plays a significant role in brain study.[149,150] While most commercial fNIRS systems are wired and large in size, the need to develop wearable and portable devices for ubiquitous monitoring of neural activities has arisen. In a similar fashion of the epidermal oximeter as shown in Figure 11a, a wearable fNIRS device implemented with IR LEDs (with

emission wavelengths such as 730, 850 nm, etc.) and Si photodiodes is mounted around the head (Figure 11e).[149] Figure 11f illustrates the temporal changes in oxygenated and deoxygenated hemoglobin levels in response to cortical stimuli.[150] With integrated arrays of detectors and LEDs placed around the entire head, the spatial image resolution of the entire brain area can be improved. Such technology can be further developed by combining fNIRS with arrays of stimulation electrodes for simultaneous neural monitoring and interrogation for future applications in neurological disease treatment and augmented brain–machine interface.

**ADVANCED
SCIENCE NEWS**

www.advancedsciencenews.com

**ADVANCED
MATERIALS**

www.advmat.de
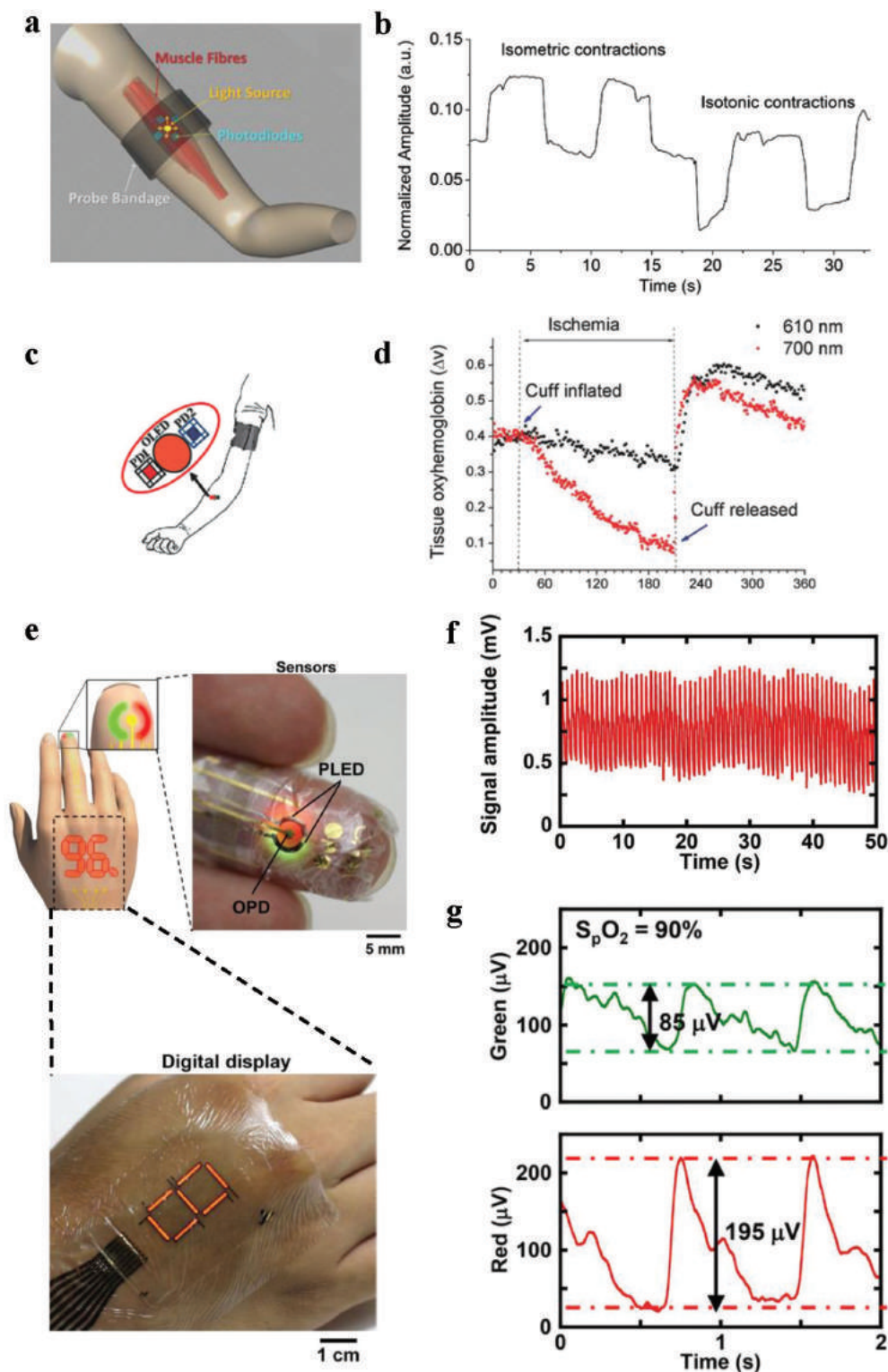
Figure 12. Organic wearable optoelectronic sensors. a) Schematic principle of a muscle contraction sensor consisting of a light source and four photodiodes on top of an arm. b) Measurement of two isometric contractions followed by two isotonic contractions. c) Schematic layout of a tissue oxygenation sensor consisting of an OLED and two photodiodes. d) Optical responses from forearm skeletal muscle of a subject, which indicate changes of tissue oxygenation at different wavelengths. a–d) Reproduced under the terms of CC-BY License.[147] Copyright 2014 The Authors, published by, Wiley-VCH. e) Smart optoelectronic e-skin system comprising pulse oximeters and displays. f) Long-term measurement of the pulse wave using a red PLED and OPD. g) Output signal from OPD with blood oxygenation. Reproduced with permission.[88] Copyright 2016, AAAS.

ADVANCED
SCIENCE NEWS
www.advancedsciencenews.com

ADVANCED
MATERIALS
www.advmat.de
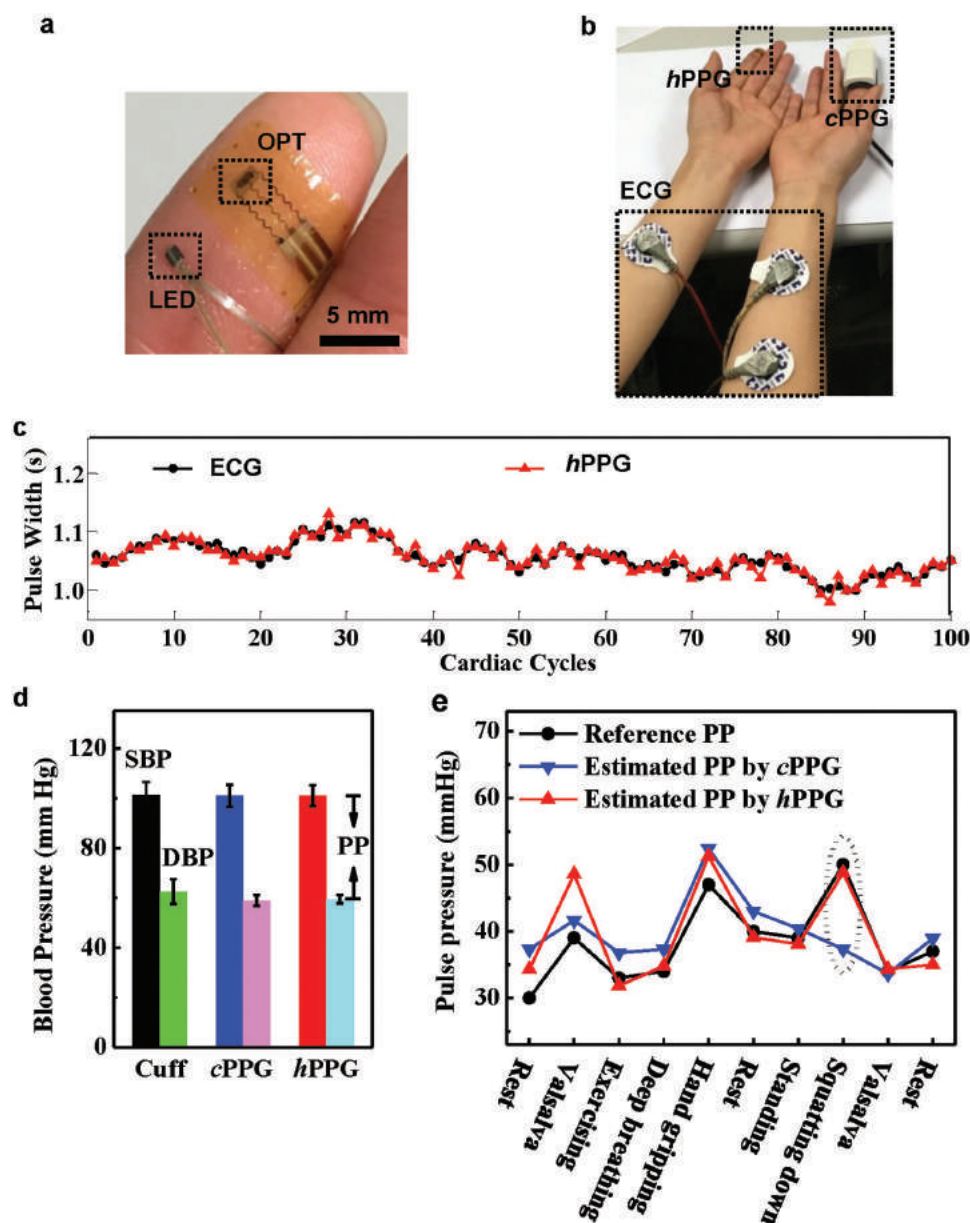
Figure 13. Organic/inorganic hybrid optoelectronic sensor. a) Photograph of an epidermal hybrid PPG sensor attached on a finger. b) Layout for monitoring health parameters. c) Tracking result of heart-rate variability conducted by the hybrid PPG sensor. c) Calculated cuffless systolic blood pressure and diastolic blood pressure. e) Tracking results of PP variation conducted by the hybrid PPG sensor. Reproduced with permission.[148] Copyright 2017, Wiley-VCH.

3.3. Implantable Sensors

In this section, we provide an overview on implantable optoelectronic devices with a focus mainly on their applications in neuroscience. In general, the penetration depth of optical signals in visible and near-IR bands into biological tissue ranges from tens of micrometers to a few millimeters. The penetration is limited due to the complicated light–biomatter interaction such as scattering and absorption.[1,151] To achieve deep-tissue light delivery (>1 cm), advanced implantable optoelectronic devices and systems are required. The direct injection of waveguides, light emitters, and detectors into the deep animal body

can potentially broaden the application in areas such as laser surgery,[152] retinal prosthetics,[153] and imaging.[154] Recent progress in the development of genetically encoded optical actuators and indicators has prompted the emergence of versatile and powerful tools for monitoring and manipulating neuronal activities both temporally and spatially.[155] In comparison with the conventional electrophysiological technique, implantable optical solution has the advantage of using light to stimulate and detect specific neuronal activities via genetic encoding.

One of the established tools for intracranial light delivery and detection is by use of implantable optical fibers (and waveguides in most cases) for deep brain optogenetic stimulation

**ADVANCED
SCIENCE NEWS**
www.advancedsciencenews.com

**ADVANCED
MATERIALS**
www.advmat.de

and fluorescence detection in vivo.[156,157] As to the optical neural interface, standard silica glass, fibers, and waveguides based on flexible, stretchable and even biodegradable materials have been thoroughly explored.[120,158–160] Recently, developed multifunctional fibers incorporate electrodes and microchannels in the microstructure to enable simultaneous optical stimulation, electrophysiological sensing, and drug delivery.[161]

As conventional implantable fibers need to interconnect with external optical and electrical components for power and signal transmission, the system is inevitably wired and large in size. Alternatively, advanced optical neural interfaces can be enabled by thin-film, microscale optoelectronic devices consisting of detectors, sensors, LEDs, and lasers based on the aforementioned design and processing strategies. These encapsulated and ultraminiaturized devices can be injected into the tissue for direct biological integration, with capabilities for multisite recording/stimulation, wireless operation, and multimodal sensing/modulation. Representative results are as shown in **Figure 14**. In this approach, an implantable optrode is formed

by integrating cellular scale InGaN blue micro-LEDs (≈50 µm × 50 µm × 5 µm in size as shown in Figure 3a) with ultrathin (<10 µm) flexible needles powered by an external flexible circuit board via RF transmission (Figure 14a).[31] With minimal invasion, such a micro-LED needle can be injected deep into the brain of freely behaving animals (Figure 14b) so as to enable the optogenetic stimulation of Channelrhodopsin-2 expressing neurons and control neural activities in vivo (Figure 14c). Furthermore, microscale neural electrodes, photodetectors, temperature sensors, and LEDs can be laminated onto one single injectable needle (Figure 14d), opening ways for real-time neural activity monitoring and biological sensing. Another breakthrough is the integration of micro-LEDs with microfluidic channels (Figure 14e) which enables simultaneous neural stimulation and drug delivery with a close-loop feedback.[162] Instead of transferring micro-LEDs onto flexible needles, our alternative is to use the implantable optrode that utilizes InGaN blue LEDs monolithically grown and fabricated on Si{111} wafers, and subsequently patterned and shaped to form
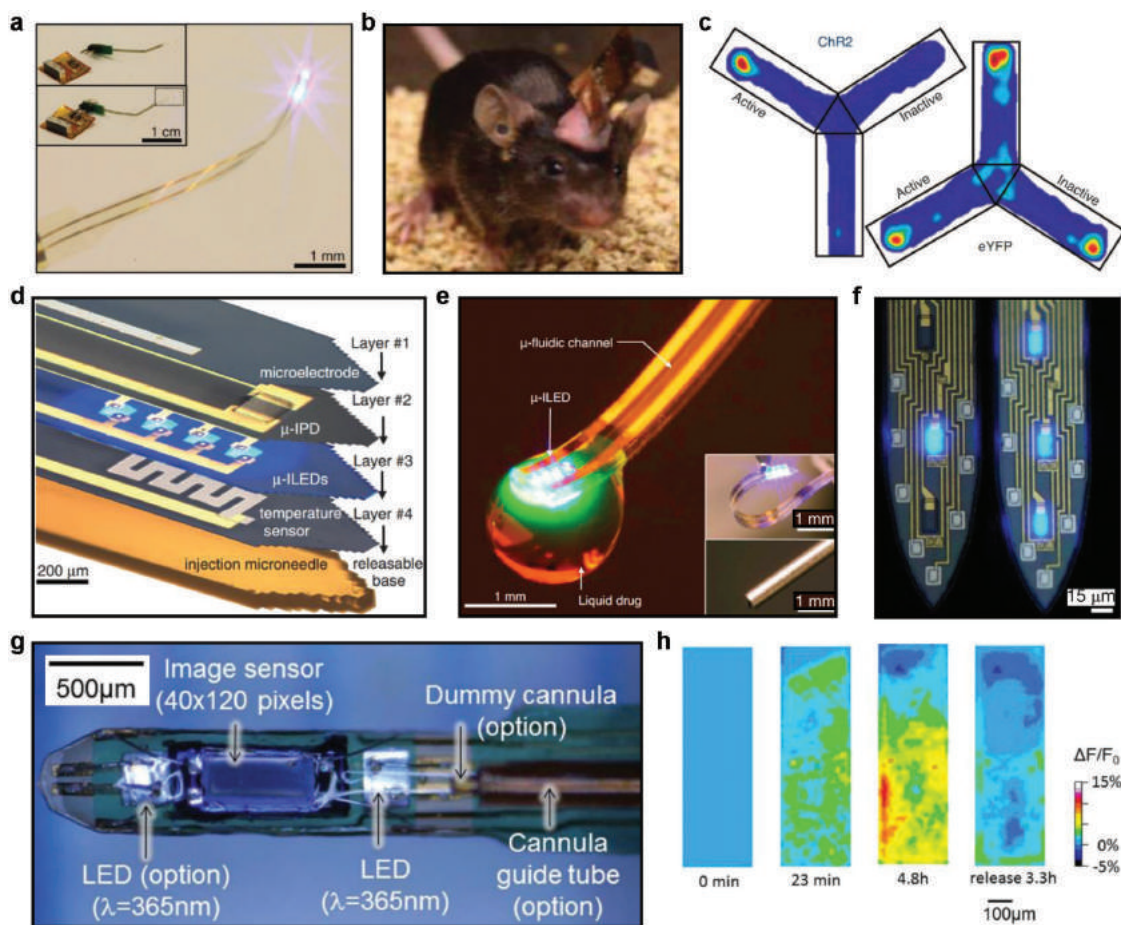

Figure 14. Representative implantable optoelectronic devices and systems for neuroscience. a) An injectable flexible needle with wirelessly powered micro-LEDs.[31] b) A freely behaving mouse with an implantable micro-LED needle.[31] c) Activity maps of ChR2 and eYFP expressing mice under optogenetic stimulation.[31] d) Scheme of a multifunctional neural probe with layers of microelectrodes, photodetectors, LEDs, and temperature sensors laminated on an injectable needle.[31] e) An injectable needle combining micro-LEDs and microfluidic channels for close-loop optogenetic modulation and drug delivery.[162] f) InGaN blue micro-LEDs monolithically integrated on Si based neural probes.[163] g) An implantable microimaging probe with micro-LEDs and a Si CMOS image sensor interconnected on a flexible substrate.[167] h) Fluorescence images obtained from the deep brain of a mouse.[167] a–d) Reproduced with permission.[31] Copyright 2013, AAAS. e) Reproduced with permission.[162] Copyright 2015, Cell Press. f) Reproduced with permission.[163] Copyright 2015, Cell Press. g,h) Reproduced with permission.[167] Copyright 2016, IEEE.

**ADVANCED
SCIENCE NEWS**
www.advancedsciencenews.com

**ADVANCED
MATERIALS**
www.advmat.de

rigid implants (Figure 14f). The advantages of these Si based neural probes is the capability to form dense micro-LED and microelectrode arrays with high scalability and spatiotemporal resolutions and the ease to implement additional metal-oxide-semiconductor (CMOS) compatible processing steps.[163] Moreover, modified tools for fluorescence detection and imaging have been developed in order to observe and understand neuronal activities in the deep brain. Conventional fluorescence imaging methods including confocal microscopy and multiphoton microscopy[164,165] only have a maximal penetration depth of a few millimeters into the brain. The problem may be addressed by inserting a glass rod based lens into the brain;[166] however, a large area of lesions can also be induced at the same time. To minimize the invasion, our approach is to combine a customized Si CMOS imaging sensor and micro-LEDs onto a flexible thin sheet so that it can be implanted into the tissue for high-resolution deep-brain fluorescence imaging.[167] The micro-LEDs adjacent to the imaging sensor serve as light sources to excite green fluorescent protein expressing cells, with an imaging sensor to capture and process fluorescence signals. Such an implantable imaging platform provides tremendous opportunities for advanced neural activity imaging as well as other biological signal sensing in the deep tissue.

3.4. Biophotonic Chips

Flexible and stretchable inorganic LEDs are applicable for biophotonic applications in areas such as optogenetics.[89,168] OLEDs have the potentiality to be the ideal light source for such applications, owing to their spectral tunability and excellent area emission property that allows high brightness with low heating effects. Park et al. applied flexible OLEDs to hyperpolarize or depolarize neurons.[168] Using microarrays of OLEDs, Steude et al. achieved real-time optical control of cell locomotion.[169,170] **Figure 15** shows a schematic illustration of OLED microarrays consisting of 320 × 720 individual blue OLEDs, each measuring 6 × 9 μm^2. The ultrathin inorganic/organic hybrid encapsulation enables a close contact between the OLEDs and the aqueous environment containing living cells. Recently, the same research team further reported that
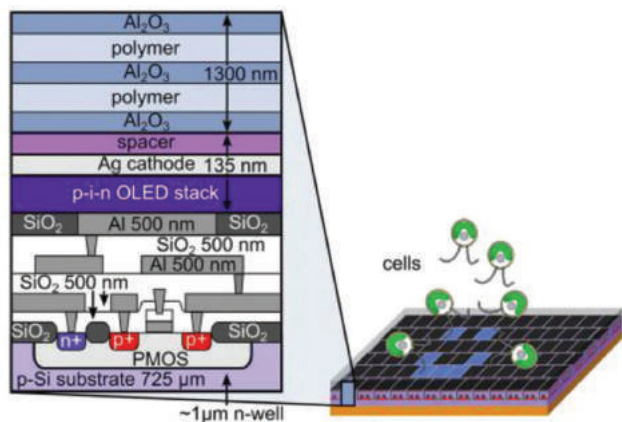
OLEDs can activate ChR in vivo for optogenetic control of Drosophila locomotor behavior.[171] These findings bring promising insights into the use of biointegrated OLEDs as light sources to control and study neuronal activities both in vitro and in vivo.

4. Summary

We have reviewed the latest development of organic- and inorganic-based optoelectronic materials, devices, and systems for biointegration. We have discussed the design and fabrication methodology to form semiconductor materials and devices in flexible and stretchable formats, the strategies to incorporate heterogeneous substrates, and interfaces and encapsulants and their applications in biomimetic, wearable, and implantable systems. Further pursuit of continued research as well as commercialization of high-performing bioinspired and biointegrated optoelectronic systems is potentially promising, e.g., the exploitations of novel low-dimension nano- and mesoscaled materials and structures with specific electronic, optical, chemical, mechanical, and thermal properties for biointegration, as well as the hybrid organic–inorganic materials and device architectures with improved performance and functionality. In order to extend the application in biomedical fields, the need for various materials, devices, and integration schemes is also eminent so as to enhance the flexibility, stretchability, biocompatibility, and degradability of the optoelectronic device. The results summarized here present great opportunities to use advanced materials and devices for novel optoelectronic systems in future biological studies and clinical applications.

Conflict of Interest

The authors declare no conflict of interest.

Figure 15. OLED microarrays for manipulation of cells with light. Reproduced with permission.[169] Copyright 2015, Wiley-VCH.

[1] S. H. Yun, S. J. J. Kwok, *Nat. Biomed. Eng.* **2017**, *1*, 0008.
[2] J. A. Rogers, *J. Am. Med. Assoc.* **2015**, *313*, 561.
[3] K. J. Yu, Z. Yan, M. Han, J. A. Rogers, *Flexible Electron.* **2017**, *1*, 4.

[4] J. A. Rogers, M. G. Lagally, R. G. Nuzzo, *Nature* **2011**, *477*, 45.

[5] J. A. Rogers, T. Someya, Y. Huang, *Science* **2010**, *327*, 1603.

[6] M. A. Meitl, Z. T. Zhu, V. Kumar, K. J. Lee, X. Feng, Y. Y. Huang, I. Adesida, R. G. Nuzzo, J. A. Rogers, *Nat. Mater.* **2006**, *5*, 33.

[7] Z. Lou, G. Z. Shen, *Adv. Sci.* **2016**, *3*, 1500287.

[8] F. Di Giacomo, A. Fakharuddin, R. Jose, T. M. Brown, *Energy Environ. Sci.* **2016**, *9*, 3007.

[9] S. Parola, B. Julián-López, L. D. Carlos, C. Sanchez, *Adv. Funct. Mater.* **2016**, *26*, 6506.

[10] H. Keum, A. Carlson, H. Ning, A. Mihi, J. D. Eisenhaure, P. V. Braun, J. A. Rogers, S. Kim, *J. Micromech. Microeng.* **2012**, *22*, 055018.

[11] H. C. Yuan, J. H. Shin, G. X. Qin, L. Sun, P. Bhattacharya, M. G. Lagally, G. K. Celler, Z. Q. Ma, *Appl. Phys. Lett.* **2009**, *94*, 013102.

[12] H. Zhou, J. H. Seo, D. M. Paskiewicz, Y. H. Zhu, G. K. Celler, P. M. Voyles, W. Zhou, M. G. Lagally, Z. Ma, *Sci. Rep.* **2013**, *3*, 1291.

[13] M. Kim, J. H. Seo, D. Zhao, S. C. Liu, K. Kim, K. Lim, W. Zhou, E. Waks, Z. Ma, *J. Mater. Chem. C* **2017**, *5*, 264.

[14] J. Yoon, A. J. Baca, S. I. Park, P. Elvikis, J. B. Geddes, L. Li, R. H. Kim, J. Xiao, S. Wang, T. H. Kim, M. J. Motala, B. Y. Ahn, E. B. Duoss, J. A. Lewis, R. G. Nuzzo, P. M. Ferreira, Y. Huang, A. Rockett, J. A. Rogers, *Nat. Mater.* **2008**, *7*, 907.

[15] J. Baca, M. Meitl, H. C. Ko, S. Mack, H. Kim, J. Dong, P. M. Ferreira, J. A. Rogers, *Adv. Funct. Mater.* **2007**, *17*, 3051.

[16] H. Kim, E. Brueckner, J. Song, Y. Li, S. Kim, C. Lu, J. D. Sulkin, K. D. Choquette, Y. Huang, R. G. Nuzzo, J. A. Rogers, *Proc. Natl. Acad. Sci. USA* **2011**, *108*, 10072.

[17] P. Kumar, S. Kanakaraju, D. L. Devoe, *Appl. Phys. A* **2007**, *88*, 711.

[18] E. Yablonovitch, T. J. Gmitter, J. P. Harbison, R. Bhat, *Appl. Phys. Lett.* **1987**, *51*, 2222.

[19] J. J. Schermer, P. Mulder, G. J. Bauhuis, M. M. J. Voncken, J. Van Deelen, E. J. Haverkamp, P. K. Larsen, *Phys. Status Solidi A* **2005**, *202*, 501.

[20] J. Yoon, S. Jo, I. S. Chun, I. Jung, H. Kim, M. Meitl, E. Menard, X. Li, J. J. Coleman, U. Paik, J. A. Rogers, *Nature* **2010**, *465*, 329.

[21] X. Sheng, C. J. Corcoran, J. He, L. Shen, S. Kim, J. Park, R. G. Nuzzo, J. A. Rogers, *Phys. Chem. Chem. Phys.* **2013**, *15*, 20434.

[22] X. Sheng, C. Robert, S. Wang, G. Pakeltis, B. Corbett, J. A. Rogers, *Laser Photonics Rev.* **2015**, *9*, L17.

[23] K. Lee, J. D. Zimmerman, X. Xiao, K. Sun, S. R. Forrest, *J. Appl. Phys.* **2012**, *111*, 033527.

[24] C. Cheng, K. Shiu, N. Li, S. Han, L. Shi, D. K. Sadana, *Nat. Commun.* **2013**, *4*, 1577.

[25] J. Zhang, G. A. De, A. Abbasi, R. Loi, J. O'Callaghan, B. Corbett, A. J. Trindade, C. A. Bower, G. Roelkens, *Opt. Express* **2017**, *25*, 14290.

[26] R. Loi, J. Ocallaghan, B. Roycroft, C. Robert, A. Fecioru, A. J. Trindade, A. Gocalinska, E. Pelucchi, C. Bower, B. Corbett, *IEEE Photonics J.* **2016**, *8*, 1504810.

[27] J. O. C. Allaghan, R. L. Oi, E. E. M. Ura, B. R. Oycroft, T. Rindade, K. T. Homas, A. G. Ocalinska, E. P. Elucchi, J. Z. Hang, R. Oelkens, C. A. B. Ower, B. Corbett, *Opt. Mater. Express* **2017**, *7*, 4408.

[28] H. Ko, K. Takei, R. Kapadia, S. Chuang, H. Fang, P. W. Leu, K. Ganapathi, E. Plis, H. S. Kim, S. Chen, M. Madsen, A. C. Ford, Y. L. Chueh, S. Krishna, S. Salahuddin, A. Javey, *Nature* **2010**, *468*, 286.

[29] W. S. Wong, T. Sands, N. W. Cheung, M. Kneissl, D. P. Bour, P. Mei, L. T. Romano, N. M. Johnson, *Appl. Phys. Lett.* **1999**, *75*, 1360.

[30] T. I. Kim, Y. H. Jung, J. Song, D. Kim, Y. Li, H. Kim, I. S. Song, J. J. Wierer, H. A. Pao, Y. Huang, J. A. Rogers, *Small* **2012**, *8*, 1643.

[31] T. I. Kim, J. G. McCall, Y. H. Jung, X. Huang, E. R. Siuda, Y. Li, J. Song, Y. M. Song, H. A. Pao, R. H. Kim, C. Lu, S. Dan Lee, I. S. Song, G. Shin, R. Al-Hasani, S. Kim, M. P. Tan, Y. Huang, F. G. Omenetto, J. A. Rogers, M. R. Bruchas, *Science* **2013**, *340*, 211.

[32] D. J. Rogers, F. H. Teherani, A. Ougazzaden, S. Gautier, L. Divay, A. Lusson, O. Durand, F. Wyczisk, G. Garry, T. Monteiro, *Appl. Phys. Lett.* **2007**, *91*, 071120.

[33] Y. Kobayashi, K. Kumakura, T. Akasaka, T. Makimoto, *Nature* **2012**, *484*, 223.

[34] K. Chung, C. Lee, G. Yi, *Science* **2010**, *330*, 655.

[35] Z. Suo, J. W. Hutchinson, *Int. J. Solids Struct.* **1989**, *25*, 1337.

[36] F. Dross, J. Robbelein, B. Vandevelde, E. Van Kerschaver, I. Gordon, G. Beaucarne, J. Poortmans, *Appl. Phys. A* **2007**, *89*, 149.

[37] S. W. Bedell, D. Shahrjerdi, B. Hekmatshoar, K. Fogel, P. A. Lauro, J. A. Ott, N. Sosa, D. Sadana, *IEEE J. Photovoltaics* **2012**, *2*, 141.

[38] S. W. Bedell, P. Lauro, J. A. Ott, K. Fogel, D. K. Sadana, *J. Appl. Phys.* **2017**, *122*, 025103.

[39] Y. Kim, S. S. Cruz, K. Lee, B. O. Alawode, C. Choi, S. Yi, J. M. Johnson, C. Heidelberger, K. Wei, S. Choi, K. Qiao, I. Almansouri, E. A. Fitzgerald, J. Kong, A. M. Kolpak, J. Hwang, J. Kim, *Nature* **2017**, *544*, 340.

[40] J. Kim, C. Bayram, H. Park, C. W. Cheng, C. Dimitrakopoulos, J. A. Ott, K. B. Reuter, S. W. Bedell, D. K. Sadana, *Nat. Commun.* **2014**, *5*, 4836.

[41] M. Ramuz, D. Leuenberger, L. Bu, *J. Polym. Sci., Part B: Polym. Phys.* **2011**, *49*, 80.

[42] S. C. B. Mannsfeld, B. C. Tee, R. M. Stoltenberg, C. V. H. Chen, S. Barman, B. V. O. Muir, A. N. Sokolov, C. Reese, Z. Bao, *Nat. Mater.* **2010**, *9*, 859.

[43] O. Ostroverkhova, *Chem. Rev.* **2016**, *116*, 13279.

[44] K. Baeg, M. Binda, D. Natali, M. Caironi, Y. Noh, *Adv. Mater.* **2013**, *25*, 4267.

[45] F. P. G. De Arquer, A. Armin, P. Meredith, E. H. Sargent, *Nat. Mater.* **2017**, *2*, 1.

[46] S. Savagatrup, A. S. Makaram, D. J. Burke, D. J. Lipomi, *Adv. Funct. Mater.* **2014**, *24*, 1169.

[47] J. Y. Oh, S. Rondeau-gagné, Y. Chiu, A. Chortos, F. Lissel, G. N. Wang, B. C. Schroeder, T. Kurosawa, J. Lopez, T. Katsumata, J. Xu, C. Zhu, X. Gu, W. Bae, Y. Kim, L. Jin, J. W. Chung, J. B. Tok, Z. Bao, *Nature* **2016**, *539*, 411.

[48] M. Shin, J. Y. Oh, K. E. Byun, Y. J. Lee, B. Kim, H. K. Baik, J. J. Park, U. Jeong, *Adv. Mater.* **2015**, *27*, 1255.

[49] J. Xu, S. Wang, G. N. Wang, C. Zhu, S. Luo, L. Jin, X. Gu, S. Chen, V. R. Feig, J. W. F. To, S. Rondeau-gagné, J. Park, B. C. Schroeder, C. Lu, J. Y. Oh, Y. Wang, Y. Kim, H. Yan, R. Sinclair, D. Zhou, G. Xue, B. Murmann, C. Linder, W. Cai, J. B. Tok, Z. Bao, *Science* **2017**, *355*, 59.

[50] A. Carlson, A. M. Bowen, Y. Huang, R. G. Nuzzo, J. A. Rogers, *Adv. Mater.* **2012**, *24*, 5284.

[51] S. I. Park, Y. Xiong, R. H. Kim, P. Elvikis, M. Meitl, D. H. Kim, J. Wu, J. Yoon, C. J. Yu, Z. Liu, Y. Huang, K. C. Hwang, F. Ferreira, X. Li, K. Choquette, J. A. Rogers, *Science* **2009**, *325*, 977.

[52] C. A. Bower, M. A. Meitl, B. Raymond, E. Radauscher, R. Cok, S. Bonafede, D. Gomez, T. Moore, C. Prevatte, B. Fisher, A. Fecioru, A. J. Trindade, R. Rotzoll, G. A. Melnik, *Photonics Res.* **2017**, *5*, A23.

[53] J. Justice, C. Bower, M. Meitl, M. B. Mooney, M. A. Gubbins, B. Corbett, *Nat. Photonics* **2012**, *6*, 610.

[54] H. Yang, D. Zhao, S. Chuwongin, J. H. Seo, W. Yang, Y. Shuai, J. Berggren, M. Hammar, Z. Ma, W. Zhou, *Nat. Photonics* **2012**, *6*, 617.

[55] D. Kang, B. Gai, B. Thompson, S. M. Lee, N. Malmstadt, J. Yoon, *ACS Photonics* **2016**, *3*, 912.

[56] D. Kang, S. M. Lee, Z. Li, A. Seyedi, J. O'Brien, J. Xiao, J. Yoon, *Adv. Opt. Mater.* **2014**, *2*, 373.

[57] X. Sheng, L. Shen, T. Kim, L. Li, X. Wang, R. Dowdy, P. Froeter, K. Shigeta, X. Li, R. G. Nuzzo, N. C Giebink, J. A. Rogers, *Adv. Energy Mater.* **2013**, *3*, 991.

[58] X. Sheng, C. A. Bower, S. Bonafede, J. W. Wilson, B. Fisher, M. Meitl, H. Yuen, S. Wang, L. Shen, A. R. Banks, C. J. Corcoran, R. G. Nuzzo, S. Burroughs, J. A. Rogers, *Nat. Mater.* **2014**, *13*, 593.

**ADVANCED
SCIENCE NEWS**

www.advancedsciencenews.com

**ADVANCED
MATERIALS**

www.advmat.de

[59] J. Lee, J. Wu, M. Shi, J. Yoon, S. I. Park, M. Li, Z. Liu, Y. Huang, J. A. Rogers, *Adv. Mater.* **2011**, *23*, 986.

[60] H. C. Ko, M. P. Stoykovich, J. Song, V. Malyarchuk, W. M. Choi, C. J. Yu, J. B. G. III, J. Xiao, S. Wang, Y. Huang, J. A. Rogers, *Nature* **2008**, *454*, 748.

[61] X. Sheng, C. Yu, V. Malyarchuk, Y. H. Lee, S. Kim, T. Kim, L. Shen, C. Horng, J. Lutz, N. C. Giebink, J. Park, J. A. Rogers, *Adv. Opt. Mater.* **2014**, *2*, 314.

[62] G. Roelkens, J. V. Campenhout, J. Brouckaert, D. V. Thourhout, R. Baets, P. R. Romeo, P. Regreny, A. Kazmierczak, C. Seassal, X. Letartre, *Mater. Today* **2007**, *10*, 36.

[63] D. H. Kim, N. Lu, R. Ma, Y. S. Kim, R. H. Kim, S. Wang, J. Wu, S. M. Won, H. Tao, A. Islam, K. J. Yu, T. I. Kim, R. Chowdhury, M. Ying, L. Xu, M. Li, H. J. Chung, H. Keum, M. McCormick, P. Liu, Y. W. Zhang, F. G. Omenetto, Y. Huang, T. Coleman, J. A. Rogers, *Science* **2011**, *333*, 838.

[64] T. Kim, J. K. Mo, Y. H. Jung, H. Jang, C. Dagdeviren, H. A. Pao, J. C. Sang, A. Carlson, K. J. Yu, A. Ameen, H. Chung, S. H. Jin, Z. Ma, J. A. Rogers, *Chem. Mater.* **2014**, *26*, 3502.

[65] K. Tanabe, K. Watanabe, Y. Arakawa, *Sci. Rep.* **2012**, *2*, 349.

[66] J. C. Sang, D. Liu, J. H. Seo, R. Dalmau, K. Kim, J. Park, D. Zhao, X. Yin, Y. H. Jung, I. K. Lee, M. Kim, X. Wang, J. D. Albrecht, W. Zhou, B. Moody, Z. Ma, https://arxiv.org/abs/1707.04223.

[67] W. Li, D. Li, G. Dong, L. Duan, J. Sun, D. Zhang, L. Wang, *Laser Photonics Rev.* **2016**, *10*, 473.

[68] B. Siegmund, A. Mischok, J. Benduhn, O. Zeika, S. Ullrich, F. Nehm, M. Böhm, D. Spoltore, H. Fröb, C. Körner, K. Leo, K. Vandewal, *Nat. Commun.* **2017**, *8*, 15421.

[69] Z.-D. Zhang, X. Gao, Y.-N. Zhong, J. Liu, L.-X. Zhang, S. Wang, J.-L. Xu, S.-D. Wang, *Adv. Electron. Mater.* **2017**, *3*, 1700052.

[70] J. Reeder, M. Kaltenbrunner, T. Ware, D. Arreaga-Salas, A. Avendano-Bolivar, T. Yokota, Y. Inoue, M. Sekino, W. Voit, T. Sekitani, T. Someya, *Adv. Mater.* **2014**, *26*, 4967.

[71] B. Peng, X. Ren, Z. Wang, X. Wang, R. C. Roberts, P. K. L. Chan, *Sci. Rep.* **2014**, *4*, 6430.

[72] A. Pierre, I. Deckman, P. B. Lechêne, A. C. Arias, *Adv. Mater.* **2015**, *27*, 6411.

[73] D. Han, Y. Khan, J. Ting, S. M. King, N. Yaacobi-Gross, M. J. Humphries, C. J. Newsome, A. C. Arias, *Adv. Mater.* **2017**, *29*, 1606206.

[74] F. C. Krebs, *Sol. Energy Mater. Sol. Cells* **2009**, *93*, 465.

[75] A. Sandström, H. F. Dam, F. C. Krebs, L. Edman, *Nat. Commun.* **2012**, *3*, 1002.

[76] P. Kopola, M. Tuomikoski, R. Suhonen, A. Maaninen, *Thin Solid Films* **2009**, *517*, 5757.

[77] D. Y. Chung, J. Huang, D. D. C. Bradley, A. J. Campbell, *Org. Electron.* **2010**, *11*, 1088.

[78] G. Pace, A. Grimoldi, D. Natali, M. Sampietro, J. E. Coughlin, G. C. Bazan, M. Caironi, *Adv. Mater.* **2014**, *26*, 6773.

[79] B.-J. de Gans, P. C. Duineveld, U. S. Schubert, *Adv. Mater.* **2004**, *16*, 203.

[80] M. Kim, H. J. Ha, H. J. Yun, I. K. You, K. J. Baeg, Y. H. Kim, B. K. Ju, *Org. Electron.* **2014**, *15*, 2677.

[81] J. Liang, L. Li, X. Niu, Z. Yu, Q. Pei, *Nat. Photonics* **2013**, *7*, 817.

[82] S. Il Park, J. H. Ahn, X. Feng, S. Wang, Y. Huang, J. A. Rogers, *Adv. Funct. Mater.* **2008**, *18*, 2673.

[83] M. Kaltenbrunner, M. S. White, E. D. Głowacki, T. Sekitani, T. Someya, N. S. Sariciftci, S. Bauer, *Nat. Commun.* **2012**, *3*, 770.

[84] G. A. Salvatore, N. Münzenrieder, T. Kinkeldei, L. Petti, C. Zysset, I. Strebel, L. Büthe, G. Tröster, *Nat. Commun.* **2014**, *5*, 2928.

[85] K. Fukuda, Y. Takeda, Y. Yoshimura, R. Shiwaku, L. T. Tran, T. Sekine, M. Mizukami, D. Kumaki, S. Tokito, *Nat. Commun.* **2014**, *5*, 4147.

[86] T. Sekitani, S. Iba, Y. Kato, Y. Noguchi, T. Someya, T. Sakurai, *Appl. Phys. Lett.* **2005**, *87*, 1.

[87] T. Sekitani, U. Zschieschang, H. Klauk, T. Someya, *Nat. Mater.* **2010**, *9*, 1015.

[88] T. Yokota, P. Zalar, M. Kaltenbrunner, H. Jinno, N. Matsuhisa, H. Kitanosako, Y. Tachibana, W. Yukita, M. Koizumi, T. Someya, *Sci. Adv.* **2016**, *2*, e1501856.

[89] R. H. Kim, D. H. Kim, J. Xiao, B. H. Kim, S. I. Park, B. Panilaitis, R. Ghaffari, J. Yao, M. Li, Z. Liu, V. Malyarchuk, D. G. Kim, A. Le, R. G. Nuzzo, D. L. Kaplan, F. G. Omenetto, Y. Huang, Z. Kang, J. A. Rogers, *Nat. Mater.* **2010**, *9*, 929.

[90] D. Yin, J. Feng, R. Ma, Y.-F. Liu, Y.-L. Zhang, X.-L. Zhang, Y.-G. Bi, Q.-D. Chen, H.-B. Sun, *Nat. Commun.* **2016**, *7*, 11573.

[91] M. Kaltenbrunner, T. Sekitani, J. Reeder, T. Yokota, K. Kuribara, T. Tokuhara, M. Drack, R. Schwödiauer, I. Graz, S. Bauer-Gogonea, S. Bauer, T. Someya, *Nature* **2013**, *499*, 458.

[92] L. Li, H. Lin, S. Qiao, Y. Zou, S. Danto, K. Richardson, J. D. Musgraves, N. Lu, J. Hu, *Nat. Photonics* **2014**, *8*, 643.

[93] S. Xu, Y. Zhang, L. Jia, K. E. Mathewson, K. I. Jang, J. Kim, H. Fu, X. Huang, P. Chava, R. Wang, S. Bhole, L. Wang, Y. J. Na, Y. Guan, M. Flavin, Z. Han, Y. Huang, J. A. Rogers, *Science* **2014**, *344*, 70.

[94] T. Sekitani, Y. Noguchi, K. Hata, T. Fukushima, T. Aida, T. Someya, *Science* **2008**, *321*, 1468.

[95] T. Sekitani, H. Nakajima, H. Maeda, T. Fukushima, T. Aida, K. Hata, T. Someya, *Nat. Mater.* **2009**, *8*, 494.

[96] Y. Wang, C. Zhu, R. Pfattner, H. Yan, L. Jin, S. Chen, F. Molina-Lopez, F. Lissel, J. Liu, N. I. Rabiah, Z. Chen, J. W. Chung, C. Linder, M. F. Toney, B. Murmann, Z. Bao, *Sci. Adv.* **2017**, *3*, e1602076.

[97] D.-H. Kim, J. Song, W. M. Choi, H.-S. Kim, R.-H. Kim, Z. Liu, Y. Y. Huang, K.-C. Hwang, Y. -w. Zhang, J. A. Rogers, *Proc. Natl. Acad. Sci. USA* **2008**, *105*, 18675.

[98] H. C. Ko, G. Shin, S. Wang, M. P. Stoykovich, J. W. Lee, D. H. Kim, J. S. Ha, Y. Huang, K. C. Hwang, J. A. Rogers, *Small* **2009**, *5*, 2703.

[99] K. Kuribara, H. Wang, N. Uchiyama, K. Fukuda, T. Yokota, U. Zschieschang, C. Jaye, D. Fischer, H. Klauk, T. Yamamoto, K. Takimiya, M. Ikeda, H. Kuwabara, T. Sekitani, Y.-L. Loo, T. Someya, *Nat. Commun.* **2012**, *3*, 723.

[100] W. Honda, T. Arie, S. Akita, K. Takei, *Sci. Rep.* **2015**, *5*, 15099.

[101] I. H. Choi, J. H. Chang, *Polym. Adv. Technol.* **2011**, *22*, 682.

[102] S.-J. Choi, S.-J. Kim, I.-D. Kim, *NPG Asia Mater.* **2016**, *8*, e315.

[103] D. Khodagholy, T. Doublet, P. Quilichini, M. Gurfinkel, P. Leleux, A. Ghestem, E. Ismailova, T. Hervé, S. Sanaur, C. Bernard, G. G. Malliaras, *Nat. Commun.* **2013**, *4*, 1575.

[104] D. J. Lipomi, M. Vosgueritchian, B. C.-K. Tee, S. L. Hellstrom, J. A. Lee, C. H. Fox, Z. Bao, *Nat. Nanotechnol.* **2011**, *6*, 788.

[105] S. H. Jeong, S. Zhang, K. Hjort, J. Hilborn, Z. Wu, *Adv. Mater.* **2016**, *28*, 5830.

[106] J. H. Seo, K. Zhang, M. Kim, D. Zhao, H. Yang, W. Zhou, Z. Ma, *Adv. Opt. Mater.* **2016**, *4*, 120.

[107] Y. Chen, H. Lin, J. Hu, M. Li, *ACS Nano* **2014**, *8*, 6955.

[108] G. Shin, A. M. Gomez, R. Alhasani, Y. R. Jeong, J. Kim, Z. Xie, A. Banks, S. M. Lee, S. Y. Han, C. J. Yoo, J. L. Lee, S. H. Lee, J. Kurniawan, J. Tureb, Z. Guo, J. Yoon, S. I. Park, S. Y. Bang, Y. Nam, M. C. Walicki, V. K. Samineni, A. D. Mickle, K. Lee, S. Y. Heo, J. G. Mccall, T. Pan, L. Wang, X. Feng, T. I. Kim, J. K. Kim, Y. Li, Y. Huang, R. W. Gereau, J. S. Ha, M. R. Bruchas, J. A. Rogers, *Neuron* **2017**, *93*, 509.

[109] J. S. Park, H. Chae, H. K. Chung, I. L. Sang, *Semicond. Sci. Technol.* **2011**, *26*, 034001.

[110] H. Fang, J. Zhao, K. J. Yu, E. Song, A. B. Farimani, C. Chiang, X. Jin, Y. Xue, D. Xu, W. Du, K. J. Seo, Y. Zhong, Z. Yang, S. M. Won, G. Fang, S. W. Choi, S. Chaudhuri, Y. Huang, M. A. Alam, J. Viventi, N. R. Aluru, J. A. Rogers, *Proc. Natl. Acad. Sci. USA* **2016**, *113*, 11682.

[111] S. W. Hwang, H. Tao, D. H. Kim, H. Cheng, J. K. Song, E. Rill, M. A. Brenckle, B. Panilaitis, S. M. Won, Y. S. Kim, Y. M. Song,

**ADVANCED
SCIENCE NEWS**
www.advancedsciencenews.com

**ADVANCED
MATERIALS**
www.advmat.de

K. J. Yu, A. Ameen, R. Li, Y. Su, M. Yang, D. L. Kaplan, M. R. Zakin, M. J. Slepian, Y. Huang, F. G. Omenetto, J. A. Rogers, *Science* **2012**, *337*, 1640.

[112] L. Yin, H. Cheng, S. Mao, R. Haasch, Y. Liu, X. Xie, S. W. Hwang, H. Jain, S. K. Kang, Y. Su, R. Li, Y. Huang, J. A. Rogers, *Adv. Funct. Mater.* **2014**, *24*, 645.

[113] S. K. Kang, G. Park, K. Kim, S. W. Hwang, H. Cheng, J. Shin, S. Chung, M. Kim, L. Yin, J. C. Lee, K. M. Lee, J. A. Rogers, *ACS Appl Mater Interfaces* **2015**, *7*, 9297.

[114] S. W. Hwang, G. Park, C. Edwards, E. A. Corbin, S. K. Kang, H. Cheng, J. K. Song, J. H. Kim, S. Yu, J. Ng, J. E. Lee, J. Kim, C. Yee, B. Bhaduri, Y. Su, F. G. Omennetto, Y. Huang, R. Bashir, L. Goddard, G. Popescu, K. M. Lee, J. A. Rogers, *ACS Nano* **2014**, *8*, 5843.

[115] S. K. Kang, S. W. Hwang, H. Cheng, S. Yu, B. H. Kim, J. H. Kim, Y. Huang, J. A. Rogers, *Adv. Funct. Mater.* **2014**, *24*, 4427.

[116] S. W. Hwang, J. K. Song, X. Huang, H. Cheng, S. K. Kang, B. H. Kim, J. H. Kim, S. Yu, Y. Huang, J. A. Rogers, *Adv. Mater.* **2014**, *26*, 3905.

[117] H. Tao, J. M. Kainerstorfer, S. M. Siebert, E. M. Pritchard, A. Sassaroli, B. J. B. Panilaitis, M. A. Brenckle, J. J. Amsden, J. Levitt, S. Fantini, D. L. Kaplan, F. G. Omenetto, *Proc. Natl. Acad. Sci. USA* **2012**, *109*, 19584.

[118] S. Nizamoglu, M. C. Gather, M. Humar, M. Choi, S. Kim, K. S. Kim, S. K. Hahn, G. Scarcelli, M. Randolph, R. W. Redmond, S. H. Yun, *Nat. Commun.* **2016**, *7*, 10374.

[119] A. Dupuis, N. Guo, Y. Gao, N. Godbout, S. Lacroix, C. Dubois, M. Skorobogatiy, *Opt. Lett.* **2007**, *32*, 109.

[120] R. Fu, W. Luo, R. Nazempour, D. Tan, H. Ding, K. Zhang, L. Yin, J. Guan, X. Sheng, *Adv. Opt. Mater.* **2018**, *6*, 1700941.

[121] M. Humar, S. H. Yun, *Nat. Photonics* **2015**, *9*, 572.

[122] J. Zimmermann, N. Jürgensen, A. J. Morfa, B. Wang, S. Tekoglu, G. Hernandezsosa, *ACS Sustainable Chem. Eng.* **2016**, *4*, 7050.

[123] H. Keum, M. Mccormick, P. Liu, Y. Zhang, F. G. Omenetto, *Science* **2011**, *333*, 838.

[124] C. Dagdeviren, Y. Shi, P. Joe, R. Ghaffari, G. Balooch, K. Usgaonkar, O. Gur, P. L. Tran, J. R. Crosby, M. Meyer, Y. Su, R. Chad Webb, A. S. Tedesco, M. J. Slepian, Y. Huang, J. A. Rogers, *Nat. Mater.* **2015**, *14*, 728.

[125] A. Koh, D. Kang, Y. Xue, S. Lee, R. M. Pielak, J. Kim, T. Hwang, S. Min, A. Banks, P. Bastien, M. C. Manco, L. Wang, K. R. Ammann, K.-I. Jang, P. Won, S. Han, R. Ghaffari, U. Paik, M. J. Slepian, G. Balooch, Y. Huang, J. A. Rogers, *Sci. Transl. Med.* **2016**, *8*, 366ra165.

[126] S. Lee, Y. Inoue, D. Kim, A. Reuveny, K. Kuribara, T. Yokota, J. Reeder, M. Sekino, T. Sekitani, Y. Abe, T. Someya, *Nat. Commun.* **2014**, *5*, 5898.

[127] H. Chung, R. H. Grubbs, *Macromolecules* **2012**, *45*, 9666.

[128] J. Li, A. D. Celiz, J. Yang, Q. Yang, I. Wamala, W. Whyte, B. R. Seo, N. V. Vasilyev, J. J. Vlassak, Z. Suo, D. J. Mooney, *Science* **2017**, *357*, 378.

[129] I. Jung, J. Xiao, V. Malyarchuk, C. Lu, M. Li, Z. Liu, J. Yoon, Y. Huang, J. A. Rogers, *Proc. Natl. Acad. Sci. USA* **2011**, *108*, 1788.

[130] Y. M. Song, Y. Xie, V. Malyarchuk, J. Xiao, I. Jung, K. J. Choi, Z. Liu, H. Park, C. Lu, R. H. Kim, R. Li, K. B. Crozier, Y. Huang, J. A. Rogers, *Nature* **2013**, *497*, 95.

[131] C. Choi, M. K. Choi, S. Liu, M. S. Kim, O. K. Park, C. Im, J. Kim, X. Qin, G. J. Lee, K. W. Cho, M. Kim, E. Joh, J. Lee, D. Son, S. H. Kwon, N. L. Jeon, Y. M. Song, N. Lu, D. H. Kim, *Nat. Commun.* **2017**, *8*, 1664.

[132] K. Zhang, Y. H. Jung, S. Mikael, J. H. Seo, M. Kim, H. Mi, H. Zhou, Z. Xia, W. Zhou, S. Gong, Z. Ma, *Nat. Commun.* **2017**, *8*, 1782.

[133] X. Xu, M. Davanco, X. Qi, S. R. Forrest, *Org. Electron.* **2008**, *9*, 1122.

[134] X. Xu, M. Mihnev, A. Taylor, S. R. Forrest, X. Xu, M. Mihnev, A. Taylor, S. R. Forrest, *Appl. Phys. Lett.* **2009**, *94*, 043313.

[135] H. Wang, H. Liu, Q. Zhao, C. Cheng, W. Hu, Y. Liu, *Adv. Mater.* **2016**, *28*, 624.

[136] H. Wang, H. Liu, Q. Zhao, Z. Ni, Y. Zou, J. Yang, L. Wang, *Adv. Mater.* **2017**, *29*, 1701772.

[137] B. C. Tee, A. Chortos, A. Berndt, A. K. Nguyen, A. Tom, A. McGuire, Z. C. Lin, K. Tien, W. G. Bae, H. Wang, P. Mei, H. H. Chou, B. Cui, K. Deisseroth, T. N. Ng, Z. Bao, *Science* **2015**, *350*, 313.

[138] M. D. Bartlett, A. B. Croll, D. R. King, B. M. Paret, D. J. Irschick, A. J. Crosby, *Adv. Mater.* **2012**, *24*, 1078.

[139] D. C. Leslie, A. Waterhouse, J. B. Berthet, T. M. Valentin, A. L. Watters, A. Jain, P. Kim, B. D. Hatton, A. Nedder, K. Donovan, *Nat. Biotechnol.* **2014**, *32*, 1134.

[140] S. A. Morin, R. F. Shepherd, S. W. Kwok, A. A. Stokes, A. Nemiroski, G. M. Whitesides, *Science* **2012**, *337*, 828.

[141] C. Yu, Y. Li, X. Zhang, X. Huang, V. Malyarchuk, S. Wang, Y. Shi, L. Gao, Y. Su, Y. Zhang, H. Xu, R. T. Hanlon, Y. Huang, J. A. Rogers, *Proc. Natl. Acad. Sci. USA* **2014**, *111*, 12998

[142] L. Gao, Y. Zhang, V. Malyarchuk, L. Jia, K. I. Jang, R. C. Webb, H. Fu, Y. Shi, G. Zhou, L. Shi, D. Shah, X. Huang, B. Xu, C. Yu, Y. Huang, J. A. Rogers, *Nat. Commun.* **2014**, *5*, 4938

[143] A. Mahmood, S. Dayeh, D. P. Butler, Z. Çelik-Butler, *Proc. IEEE Sens.* **2003**, *2*, 777.

[144] W. Gao, S. Emaminejad, H. Y. Y. Nyein, S. Challa, K. Chen, A. Peck, H. M. Fahad, H. Ota, H. Shiraki, D. Kiriya, D. H. Lien, G. A. Brooks, R. W. Davis, A. Javey, *Nature* **2016**, *529*, 509

[145] J. Kim, G. A. Salvatore, H. Araki, A. M. Chiarelli, Z. Xie, A. Banks, X. Sheng, Y. Liu, J. W. Lee, K. I. Jang, S. Y. Heo, K. Cho, H. Luo, B. Zimmerman, J. Kim, L. Yan, X. Feng, S. Xu, M. Fabiani, G. Gratton, Y. Huang, U. Paik, J. A. Rogers, *Sci. Adv.* **2016**, *2*, e1600418.

[146] C. M. Lochner, Y. Khan, A. Pierre, A. C. Arias, *Nat. Commun.* **2014**, *5*, 5745.

[147] A. K. Bansal, S. Hou, O. Kulyk, E. M. Bowman, I. D. W. Samuel, *Adv. Mater.* **2015**, *27*, 7638.

[148] H. Xu, J. Liu, J. Zhang, G. Zhou, N. Luo, N. Zhao, *Adv. Mater.* **2017**, *29*, 1700975.

[149] R. Mckendrick, R. Parasuraman, H. Ayaz, *Front. Syst. Neurosci.* **2015**, *9*, 27.

[150] M. Ferrari, V. Quaresima, *NeuroImage* **2012**, *63*, 921.

[151] P. N. Prasad, *Introduction to Biophotonics*, Wiley-Interscience, Hoboken, NJ **2003**.

[152] J. Marshall, S. L. Trokel, S. Rothery, R. R. Krueger, *Ophthalmology* **1988**, *95*, 1411.

[153] K. Mathieson, J. Loudin, G. Goetz, P. Huie, L. Wang, T. I. Kamins, L. Galambos, R. Smith, J. S. Harris, A. Sher, *Nat. Photonics* **2012**, *6*, 391.

[154] S. A. Boppart, R. Richards-Kortum, *Sci. Transl. Med.* **2014**, *6*, 253rv2.

[155] M. R. Warden, J. A. Cardin, K. Deisseroth, *Annu. Rev. Biomed. Eng.* **2014**, *16*, 103.

[156] K. Deisseroth, *Nat. Methods* **2011**, *8*, 26.

[157] L. A. Gunaydin, L. Grosenick, J. C. Finkelstein, I. V. Kauvar, L. E. Fenno, A. Adhikari, S. Lammel, J. J. Mirzabekov, R. D. Airan, K. A. Zalocusky, K. M. Tye, P. Anikeeva, R. C. Malenka, K. Deisseroth, *Cell* **2014**, *157*, 1535.

[158] M. Choi, J. W. Choi, S. Kim, S. Nizamoglu, S. K. Hahn, S. H. Yun, *Nat. Photonics* **2013**, *7*, 987.

[159] C. Lu, U. P. Froriep, R. A. Koppes, A. Canales, V. Caggiano, J. Selvidge, E. Bizzi, P. Anikeeva, *Adv. Funct. Mater.* **2015**, *24*, 6594.

[160] C. Lu, S. Park, T. J. Richner, A. Derry, I. Brown, C. Hou, S. Rao, J. Kang, C. T. Mortiz, Y. Fink, P. Anikeeva, *Sci. Adv.* **2017**, *3*, e1600955.

[161] A. Canales, X. Jia, U. P. Froriep, R. A. Koppes, C. M. Tringides, J. Selvidge, C. Lu, C. Hou, L. Wei, Y. Fink, P. Anikeeva, *Nat. Biotechnol.* **2015**, *33*, 277

[162] J. W. Jeong, J. G. McCall, G. Shin, Y. Zhang, R. Al-Hasani, M. Kim, S. Li, J. Y. Sim, K. I. Jang, Y. Shi, D. Y. Hong, Y. Liu, G. P. Schmitz, L. Xia, Z. He, P. Gamble, W. Z. Ray, Y. Huang, M. R. Bruchas, J. A. Rogers, *Cell* **2015**, *162*, 662

[163] F. Wu, E. Stark, P. C. Ku, K. D. Wise, G. Buzsáki, E. Yoon, *Neuron* **2015**, *88*, 1136.

[164] J. B. Pawley, *Handbook of Biological Confocal Microscopy*, Plenum Press, New York **1995**.

[165] F. Helmchen, W. Denk, *Nat. Methods* **2005**, *2*, 932.

[166] B. A. Flusberg, A. Nimmerjahn, E. D. Cocker, E. A. Mukamel, R. P. Barretto, T. H. Ko, L. D. Burns, J. C. Jung, M. J. Schnitzer, *Nat. Methods* **2008**, *5*, 935.

[167] J. Ohta, Y. Ohta, H. Takehara, T. Noda, K. Sasagawa, T. Tokuda, M. Haruta, T. Kobayashi, Y. M. Akay, M. Akay, *Proc. IEEE* **2017**, *105*, 158.

[168] S. I. Park, D. S. Brenner, G. Shin, C. D. Morgan, B. A. Copits, H. U. Chung, M. Y. Pullen, K. N. Noh, S. Davidson, S. J. Oh, J. Yoon, K.-I. Jang, V. K. Samineni, M. Norman, J. G. Grajales-Reyes, S. K. Vogt, S. S. Sundaram, K. M. Wilson, J. S. Ha, R. Xu, T. Pan, T. Kim, Y. Huang, M. C. Montana, J. P. Golden, M. R. Bruchas, R. W. Gereau, J. A. Rogers, *Nat. Biotechnol.* **2015**, *33*, 1280.

[169] A. Steude, M. Jahnel, M. Thomschke, M. Schober, M. C. Gather, *Adv. Mater.* **2015**, *27*, 7657.

[170] A. Steude, E. C. Witts, G. B. Miles, M. C. Gather, *Sci. Adv.* **2016**, *2*, e1600061.

[171] A. Morton, C. Murawski, S. R. Pulver, M. C. Gather, *Sci. Rep.* **2016**, *6*, 31117.

1800156 (22 of 22)